LIMNOLOGY
and
OCEANOGRAPHY

ASLO

Limnol. Oceanogr. 60, 2015, 553–572

doi: 10.1002/lno.10035

Methane oxidation pathways and associated methanotrophic communities in the water column of a tropical lake

Prosper K. Zigah,*[1] Kirsten Oswald,[1,2] Andreas Brand,[1,2] Christian Dinkel,[1] Bernhard Wehrli,[1,2] Carsten J. Schubert[1]

[1]Department of Surface Waters—Research and Management, Swiss Federal Institute of Aquatic Science and Technology (Eawag), Kastanienbaum, Switzerland

[2]Institute of Biogeochemistry and Pollutant Dynamics, Department of Environmental System Science, Swiss Federal Institute of Technology (ETH), Zurich, Switzerland

Abstract

We examined methane (CH_4) oxidation pathways and associated methanotrophic communities in the water column of Lake Kivu using abundance and isotopic compositions of CH_4 and phospholipid fatty acids (PLFA), distributions of glycerol dialkyl glycerol tetraethers, and catalyzed reporter deposition fluorescence in situ hybridization (CARD–FISH) analysis. The carbon isotopic data of CH_4 indicate that aerobic CH_4 oxidation is the predominant pathway of microbial CH_4 consumption with an isotopic fractionation factor (α) of 1.022–1.038. A small amount of CH_4 is oxidized anaerobically, with an α of 1.002–1.006. Aerobic CH_4 oxidation is mediated by type II methane–oxidizing bacteria (type II MOB) based on the ^{13}C depletion ($\delta^{13}C$ of $-40.5‰$ to $-43.7‰$) of diagnostic C18:1ω7 fatty acids in the surface waters. CARD–FISH images and PLFA components C16:1ω7 and C16:1ω5 indicate the presence of type I MOB in the methane and nutrient–rich deep–water region. ^{13}C depletion of C16:1ω7 and C16:1ω5 ($\delta^{13}C$, $\sim -40‰$ to $-50.6‰$) in the lake water below 52 m suggests the involvement of type I MOB in methane oxidation in the anoxic deep–water regions of the lake. A novel cluster of anaerobic methane–oxidizing archaea (ANME) rather than the known ANME–1 and ANME–2 appear to be involved in anaerobic oxidation of methane (AOM). Sulfate reducing bacteria are associated with AOM in the lake based on the ^{13}C depletion ($\delta^{13}C$, $-38.2‰$ to $-45.0‰$) of *anteiso*–methyl–C15:0 fatty acid. Methane constitutes an important carbon and energy source (up to 38%) for the heterotrophic and autotrophic communities in the lake.

The emission of CH_4 from freshwater lakes (estimated at 8–48 Tg CH_4 per annum) constitutes an important component of the global CH_4 budget (about 6–16% of annual global CH_4 emissions; Bastviken et al. 2004) and is higher than the annual CH_4 emissions from the oceans (2% of annual global CH_4 emissions; Reeburgh 2007). The amount of CH_4 emitted from freshwater and marine systems to the atmosphere is just a small fraction of the CH_4 produced in these systems as microbially mediated CH_4 oxidation in the sediments and water columns of these systems mitigates CH_4 flux to the atmosphere. Studies show that $\sim$ 80–90% of CH_4 produced in freshwater and marine systems is degraded or removed through anaerobic and aerobic CH_4 oxidation (Reeburgh 2007).

Anaerobic oxidation of methane (AOM) can be driven by sulfate as the electron acceptor and is mediated by anaerobic methane–oxidizing archaea (ANME) alone (Milucka et al. 2012) or ANME in a consortium with sulfate reducing bacteria (SRB) (Boetius et al. 2000); this process has been observed in sediments and water columns of marine aquatic systems (Knittel and Boetius 2009). Alternative electron acceptors such as nitrate (Ettwig et al. 2008; Haroon et al. 2013) and nitrite (Ettwig et al. 2010) have been observed to oxidize CH_4 in sediments but not in the water columns of aquatic systems, whereas iron and manganese have been observed in the sediments (Beal et al. 2009) and water columns (Crowe et al. 2011).

In contrast to AOM, aerobic methane–oxidizing bacteria (MOB) mediate CH_4 oxidation using molecular oxygen (O_2) as the terminal electron acceptor (Hanson and Hanson 1996), and the process is thought to be influenced by the concentrations of dissolved CH_4, oxygen, copper, and inorganic nitrogen. Previous studies in the water columns of freshwater lakes have reported a half–saturation constant (the concentration needed for oxidation rate of one–half of the maximum rate) of 17–25 μmol O_2 L^{-1} and optimal

*Correspondence: zigah004@umn.edu

oxygen concentrations of 3–31 μmol L^{-1} for aerobic microbial CH_4 oxidation (Lidstrom and Somers 1984). Also, Rudd and Hamilton (1979) in their study of CH_4 cycling in Lake 227 in Ontario, Canada observed that aerobic methanotrophs fix nitrogen when dissolved inorganic nitrogen (DIN) concentrations were below 3 μmol L^{-1}. Therefore, because of the requirements of low oxygen, as well as high CH_4 and DIN concentrations, MOB typically oxidize CH_4 at the oxic-anoxic boundaries in aquatic ecosystems. MOB are differentiated into type I, type X, and type II based on several characteristics or properties such as membrane arrangement, optimal growth temperature, predominant membrane phospholipids, and pathway of carbon assimilation (Hanson and Hanson 1996). Type I MOB belongs to the gammaproteobacteria and uses the ribulose monophosphate (RuMP) pathway for assimilating carbon. Also, the membrane lipids of type I MOB are dominated by C16 phospholipid fatty acids (PLFA). In contrast, type II MOB belong to the alphaproteobacteria and utilize the serine pathway for carbon assimilation. The membrane lipids of type II MOB are predominantly C18 PLFA (Hanson and Hanson 1996).

As methane is typically highly ^{13}C-depleted, methanotrophic bacteria and archaea directly consuming CH_4 synthesize cell membranes and constituent PLFA and glycerol ethers that are highly ^{13}C-depleted. Consequently, carbon isotopic signatures of bacteria-derived PLFA and archaea-derived archaeol and glycerol dialkyl glycerol tetraethers (GDGTs) have been useful for identifying and/or characterizing the organisms involved in CH_4 oxidation in aquatic environments. For instance, Blumenberg et al. (2004) used the ^{13}C-depletion ($\delta^{13}C$ of $-108‰$ to $-75‰$) of pentamethylicosane, archaeol, GDGTs, and PLFA to characterize the bacteria and archaea involved in anaerobic CH_4 oxidation in sediments from the Black Sea.

In addition to the lipid biomarkers, others have used cell counting or labeling approaches such as fluorescence in situ hybridization (FISH) and catalyzed reporter deposition fluorescence in situ hybridization (CARD-FISH) to characterize methanotrophic (and methanogenic) communities in aquatic environments (Llirós et al. 2010; Schubert et al. 2011). Most of these studies (both molecular isotopic and labeling approaches discussed above) have focused on marine systems with just few studies from the water columns of tropical lakes, including Lake Matano (Crowe et al. 2011), Lake Tanganyika (Durisch–Kaiser et al. 2011), and Lake Kivu (Pasche et al. 2011).

Lake Kivu is a meromictic lake in the East African Rift Valley, located between the Republic of Rwanda and the Democratic Republic of Congo. The anoxic monimolimnion is permanently separated from the surface waters and contains an unusually high amount of dissolved CH_4 ($\sim$ 60 km^3 of CH_4 at standard temperature and pressure; Schmid et al. 2005). The very high CH_4 concentrations in the lake (up to 20 mmol L^{-1}; Schmid et al. 2005) make Lake Kivu an ideal system for investigating the microbial communities involved in CH_4 oxidation in aquatic environments. CH_4 oxidation rates in Lake Kivu have previously been examined by Jannasch (1975) and Pasche et al. (2011) and reported to be 31–33 g C m^{-2} yr^{-1}. Although Llirós et al. (2012) provided important insights into the general microbial ecology of the lake, the microbial communities involved in CH_4 oxidation in the lake have only been examined by Pasche et al. (2011). Using particulate CH_4 monooxygenase (*pmoA*) gene analysis, Pasche et al. (2011) reported that a type X MOB (*Methylococcus capsulatus*) was involved in aerobic methane oxidation in the lake, although they also pointed out that their primer set has a potential bias toward type X MOB and that diverse communities could be involved in aerobic methane oxidation in the lake. Also, Pasche et al. (2011) used denaturing gradient gel electrophoresis (DGGE) and methyl coenzyme M reductase (*mcrA*) gene analysis and noted that the SRB *Desulfocapsa* and an ANME *Methanomicrobiales* may be involved in anaerobic methane oxidation coupled to sulfate reduction in the anoxic region of the water column.

In this study, we sought to enhance our understanding of the methane oxidation pathways and methanotrophic communities in Lake Kivu using compound-specific isotope analysis and microscopy. We addressed the following research questions in Lake Kivu: (1) What is the predominant pathway of CH_4 oxidation in the water column? (2) How much CH_4 is entering the food web of the lake? (3) Which aerobic methanotrophs are mainly responsible for most of the CH_4 oxidation in the oxic zone? and (4) Which microbial communities are involved in AOM in the lake? We used concentration and carbon isotopic composition of dissolved CH_4 (and dissolved inorganic carbon [DIC]) to examine the predominant pathway (aerobic vs. anaerobic) of CH_4 oxidation in the lake. The carbon isotopic composition of biomarkers of heterotrophic (and autotrophic) organisms including phytol (3,7,11,15-tetramethyl-2-hexadecen-1-ol), brassicasterol (24-methyl cholest-5,22-dien-3β-ol), dinosterol (4α,23,24-trimethyl-5α-cholest-22E-en-3β-ol), and cholesterol (cholest-5-en-3β-ol) (Wakeham et al. 1997; Schubert et al. 1998) was used to determine whether CH_4 is a significant carbon and energy source for the lake food web. Finally, the microbial communities associated with CH_4 oxidation in the lake were characterized from a detailed vertical profile of suspended particulate matter (SPM) from the lake water column by using CARD-FISH and the distribution and carbon isotopic composition of PLFA, archaeol (2,3-Di-O-phytanyl-*sn*-glycerol) and glycerol diakyl glycerol tetraethers (GDGTs).

Methods

Study site

Lake Kivu has a surface area of 2370 km^2 and is one of the deep lakes in the East African Rift Valley, with a maximum depth and volume of 485 m and 580 km^3, respectively.

The lake is surrounded by active volcanoes (e.g., Nyirangogo in DR Congo) and is fed by subaquatic springs entering the lake at different depths below 120 m water depth (Schmid et al. 2005). Approximately 130 rivers within the lake catchment feed the lake with $\sim$ 2.4 km^3 yr^{-1} of water (Muvundja 2010). The lake is meromictic with the oxic mixolimnion at $\sim$ 30 m in the rainy season (September–May) and 60 m in the dry windy season (June–August). The anoxic monimolimnion has a hydrologic residence time of 800–1000 years and is rich in nutrients and dissolved CH_4 (Schmid et al. 2005). Most of the CH_4 in the lake ($\sim$ 65%) is thought to be of geogenic origin (Pasche et al. 2009). Primary production in the lake is dominated by diatoms during the dry season and by cyanobacteria during the rainy season (Sarmento et al. 2012). Based on phylogenetic analysis of planktonic archaea, most of the Euryarchaeota in the deep anoxic waters are reported to belong to methanogenic lineages (Methanosarcinales and Methanocellales) (Llirós et al. 2010).

Previous investigations across the various provinces of the lake show that the offshore regions of the main basin of Lake Kivu are homogeneous, exhibiting little horizontal variability in terms of trace metals (e.g., zinc, copper, iron, and manganese) and physicochemical properties (e.g., temperature, pH, dissolved organic carbon, dissolved oxygen) (Julius 2011). Other properties that are similar in different regions of the lake include the chlorophyll concentration and primary production (Sarmento et al. 2012), nutrient concentrations and internal recycling (Pasche et al. 2009), as well as CH_4 concentrations and emissions (Borges et al. 2011), and distribution of crenarchaeota and methanogens (Llirós et al. 2010). The aerobic CH_4 oxidation rate has been estimated at 31–33 g C m^{-2} yr^{-1} (Jannasch 1975; Pasche et al. 2011), and CH_4 emission rates amount to as little as 0.01 g C m^{-2} yr^{-1} (Borges et al. 2011). Sulfate (SO_4^{2-}) concentration is reported to be $\sim$ 0.15 mmol L^{-1} in the oxic surface waters and decreases sharply from 0.14 mmol L^{-1} to 0.01 mmol L^{-1} between 60 m and 90 m, with values below detection at 100 m (Pasche et al. 2009). Previous studies have reported methane $\delta^{13}C$ values of $\sim -60‰$ below 90 m, increasing to $-43‰$ in the oxic surface waters in the lake (Pasche et al. 2011).

Sample collection

The lake was sampled from the permanent sampling platform kept by the Lake Kivu Monitoring Program, Ministry of Infrastructure, Gisenyi, Rwanda (1.074°S, 22.226°N; Fig. 1) between 14 January 2013 and 30 January 2013. This site at the northern main basin of the lake (total water depth $\sim$ 350 m) was chosen to take advantage of the data from adjacent sediment trap moorings. Depth profiles of temperature, conductivity, pH, and turbidity were obtained in situ with a RBR multiparameter probe (RBR XRX-620). Water samples for CH_4 concentration and CH_4 stable carbon isotopic composition ($\delta^{13}C$–CH_4) were transferred directly from the Niskin bottle into precleaned 120 mL serum bottles by rinsing twice with sample and then overflowing with two volumes of the sample. Samples were immediately poisoned with cupric chloride ($CuCl_2$; Pasche et al. 2011), and sealed airtight with butyl–rubber stoppers and aluminum crimp caps. All samples were measured within six weeks of collection.

Water samples for DIC concentration were collected by overflowing two volumes of the lake water into 1 L precombusted ($\geq$ 4 h at 450°C) glass bottles; aliquots of these samples were immediately filtered via 20 mL syringe and syringe–filters (Millex-GP PES membrane, 0.22 μm pore size) into 12 mL air-tight exetainers and preserved with cupric chloride (Pasche et al. 2011). For measuring stable carbon isotopes of DIC ($\delta^{13}C$-DIC), $\sim$ 1-mL aliquots of syringe-filtered water were collected directly into air-tight capped 12 mL exetainers prefilled with $\sim$ 0.5 mL of concentrated phosphoric acid and preflushed with helium gas to remove carbon dioxide. DIC and $\delta^{13}C$-DIC samples were kept cool in the dark until analyses. DIC samples were measured within four weeks of collection.

SPM samples were obtained using an in situ filtration device (Water Transfer System; McLane Laboratories) to filter 41–135 L of lake water through precombusted double-packed Whatman GF/F filters (142 mm diameter; 0.7 μm nominal pore size). The filters with the retained particulate matter (SPM sample) were folded and placed in previously combusted aluminum foil and stored frozen at -20°C until analysis. To ensure that the SPM samples remained frozen during transport (by air) to Switzerland, the frozen filters were stored between frozen cooling elements in a cooler.

Measurement of dissolved O_2, S(-II), NH_4^+, and NO_2^-

Oxygen concentrations were measured in situ using needle-type optodes (Presens). Winkler concentrations were 237.5 ± 6.3 μmol L^{-1} at 2 m depth and were used to calibrate the optodes. The optode logging system consisted of a EOM-O2-mini transducer (Presens), which was recorded by an additional data logger (Schmid Engineering). Details on the electrodes and logging system can be found in Kirf et al. (2014). The detection limit of the trace oxygen probe was 0.02 μmol L^{-1}. Concentrations of S(-II), NH_4^+, and NO_2^- were measured in lake water from selected depths using standard protocols as described by Pasche et al. (2009).

Measurements of CH_4 and DIC concentrations

CH_4 concentrations were measured by the headspace analysis. In brief, a headspace of 30 mL was created with N_2 gas; after equilibration in an ultrasonic bath with the samples stored upside down, the CH_4 concentration in the headspace was measured on a gas chromatograph (GC; Agilent 6890) with a flame ionization detector (FID). DIC concentration was measured on a Shimadzu total organic carbon (Shimadzu TOC-$L_{CSH/CPH}$) analyzer. The analyzer was calibrated with primary-standard grade sodium carbonate and sodium bicarbonate. The inorganic carbon in the sample was

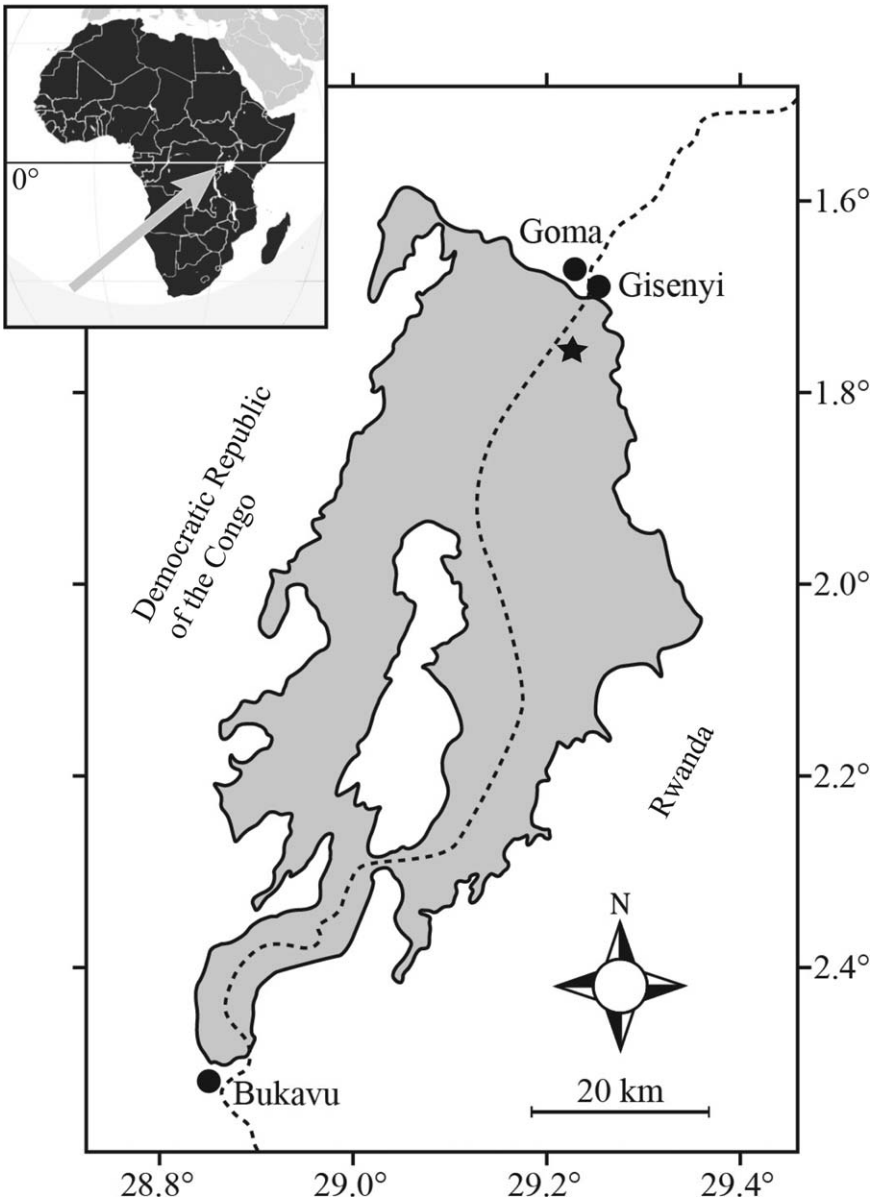

Fig. 1. Map of Lake Kivu showing sampling site (star symbol) in the main basin of the lake.

volatilized with 25% (by weight) phosphoric acid in a CO_2-free closed reaction vessel and the evolved CO_2 was measured by a nondispersive infrared detector.

Measurement of stable carbon isotopes of CH_4, DIC, and SPM

Stable carbon isotope distributions in CH_4 samples were measured using an Isoprime isotope ratio mass spectrometer (IRMS) coupled to a trace gas preconcentrator (Micromass UK). An in-house CH_4 standard was analyzed at the beginning and after every four samples to assess instrumental performance. Isotopic ratios are reported in the standard delta notation relative to Vienna Pee Dee Belemnite. Instrumental precision based on multiple analyses of this CH_4 standard was $\sim 0.5‰$. The stable carbon isotopic composition of DIC was measured using a GasBench II coupled to a Delta V IRMS with a ConFlo IV interface (Thermo Fisher Scientific). Typical instrumental precision based on multiple analyses of an external standard was 0.2‰. SPM samples were freeze-dried, homogenized, and fumigated with 12 mol L^{-1} HCl overnight to remove carbonate; they were then oven-dried at 60°C and cooled in a dessicator. Portions were loaded into tin capsules and analyzed for stable carbon ($\delta^{13}C$) and nitrogen ($\delta^{15}N$) isotopes on an elemental analyzer (EA) coupled to an Isoprime IRMS (Micromass). The EA-IRMS was calibrated with acetanilide (Merck), sulfanilic acid (Sigma Aldrich), and

an in-house sediment standard. Typical instrumental precision based on multiple analyses of external standards was 0.2‰ for $\delta^{13}C$ and 0.3‰ for $\delta^{15}N$.

Lipid biomarker analyses

SPM samples were extracted with methylene chloride (DCM) and methanol (MeOH) (DCM : MeOH 7 : 3, v : v) by microwave digestion (MLS 1200 Mega) to obtain total lipid extracts. The lipid extract was eluted over an activated copper (Cu) column to remove elemental sulfur (S) and through a sodium sulfate (Na_2SO_4) column to remove water. The extracts were saponified with 1 mol L^{-1} potassium hydroxide (KOH) in MeOH at 80°C for 3 h. The neutral fraction was extracted from the combined (H_2O–MeOH–KOH) phase with hexane, and the acid fraction was extracted from the aqueous phase with hexane after adding 6 mol L^{-1} HCl to bring the pH to < 2. The acid and neutral fractions were each dried over a Na_2SO_4 column. The neutral fraction was further separated into polar and apolar fractions using an NH_2 column (6 mL Glass; 500 mg sorbent).

The polar fraction containing the alcohols was derivatised to trimethylsilyl ester form (TMS) by silylation (80°C for 30 min) with N,O-bis(trimethylsilyl)trifluoroacetamide (BSTFA; Supelco). The fatty acids were derivatised via methylation (60°C for 30 min) with 10% Boron trifluoride-methanol solution (Sigmal Aldrich) to produce fatty acid methyl esters (FAMES). Double bond positions in FAMES were determined from analysis of dimethyldisulfide (DMDS) adducts. Individual compounds were identified on a gas chromatograph-mass spectrometer (Shimadzu GC-MS) using the following instrumentation and settings: GC-2010 Plus coupled to GCMS QP 2010 with GC column (ZB-5MS, Phenomenex) specifications of 30 m × 0.25 mm inner diameter × 0.25 μm film thickness. Carrier gas (helium) flow rate of 1.49 mL min^{-1} and a temperature program (70°C to 130°C at 20°C min^{-1}, and then at 4°C min^{-1} to 320°C, and held at 320°C for 20 min) were used. FAMES were quantified using external calibration on a GC with a FID (Shimadzu GC-FID, GC-2010 Plus with auto injector, AOC-20i) with GC column (ZB-5MS, Phenomenex) dimensions of 0.25 mm inner diameter, 0.25 μm film thickness and a length of 30 m. Carrier gas (helium) flow rate of 2 mL min^{-1} and a temperature program (70°C to 150°C at 10°C min^{-1}, and then at 5°C min^{-1} to 290°C, and held at 290°C for 20 min) were used. Quantification of alcohols was also performed using the same GC-FID with the same GC column, but the final temperature was increased to 320°C and held for 13 min. Typical precision of biomarker analyses was ≤ 4% based on multiple analyses of an external standard.

For GDGT analysis, neutral fractions were separated over a silica column using hexane : DCM (9 : 1, v : v) and DCM : MeOH (1 : 1, v : v) to produce apolar and polar fractions, respectively. The polar fraction was dried under N_2, dissolved in hexane : isopropanol (99 : 1, v : v) and filtered over a 0.45 μm polytetrafluoroethylene (PTFE) filter prior to analysis. For absolute quantification, a synthesized standard (C_{46} GDGT) was added to each sample before analysis. GDGT compounds were separated using a high performance liquid chromatograph-mass spectrometer (HPLC-MS) with atmospheric pressure chemical ionization (APCI; Agilent 1260 Infinity series) and using a Grace Prevail Cyano column (150 mm × 2.1 mm; 3 μm). The GDGTs were eluted isocratically with 90% hexane and 10% hexane : isopropanol (9 : 1, v : v) for 5 min and then with a linear gradient to 18% hexane : isopropanol (9 : 1, v : v) over 34 min with a flow rate of 0.2 mL min^{-1}.

Compound-specific isotope analyses (CSIA)

Compound-specific carbon isotopic compositions ($\delta^{13}C$) of FAMES and silylated alcohols were analyzed on an Isoprime IRMS coupled to a GC (Agilent 6890N) with a combustion interface. The extracted compounds were dissolved in ethyl acetate prior to separation by GC using the same GC column and temperature programs used for the quantification of the compounds by GC-FID. Samples were analyzed in duplicate. In-house standards (methyl stearate and heptadecane) with known $\delta^{13}C$ were used to assess and correct for isotopic fractionation during GC separation. Measured $\delta^{13}C$ values of compounds were also corrected for methyl and trimethyl carbon introduced during derivatization via isotopic-mass balance calculation. Instrumental precision of $\delta^{13}C$ based on duplicate analyses was ≤ 1‰.

Calculations of biomarker source and isotope fractionation

The contribution of CH_4-derived carbon or methanotrophic bacterial biomass to biomarkers including phytol (non-specific phytoplankton including cyanobacteria), dinosterol (diatoms and dinoflagellates), brassicaterol (diatoms), and cholesterol (e.g., zooplankton) was estimated using a binary (CH_4-derived carbon and non-CH_4-derived carbon) mixing model as follows:

$$\delta^{13}C_{Biomarker} = f \bullet \delta^{13}C_{CH_4-C} + (1-f) \bullet \delta^{13}C_{NonCH_4-C} \quad (1)$$

where f denotes the fraction of CH_4-derived carbon in the biomarker, (1 - f) stands for the fraction of non-CH_4 carbon in the biomarker, and the subscripts "CH_4—C" and "Non CH_4—C" refer to methane-derived carbon and non-methane carbon, respectively. We used a $\delta^{13}C$ value of −78‰ as the methane-derived carbon endmember based on our measured deep-water (200 m) methane $\delta^{13}C$ of −62‰ and assuming a fractionation of −16‰ (Summons et al. 1994; Bastviken et al. 2003). For the non-methane carbon endmember, we used a $\delta^{13}C$ value of −23‰ computed from the $\delta^{13}C$ value of $CO_{2(aq)}$ (−6‰ based on our measured average surface water [< 40 m] DIC-$\delta^{13}C$ of ∼ 4‰ as $CO_{2(aq)}$ is typically ^{13}C-depleted by ∼ 10‰ relative to the bulk DIC; McCallister and del Giorgio 2008) and assuming an algal photosynthetic fractionation of 17‰. We did not use the typical C_3 algal

Table 1. CARD-FISH probes used in this study along with their specificity, applied permeabilization, % (v : v) formamide in the hybridization buffer, and reference.

Probe	Specificity	Permeabilization	% formamide	Probe sequence (5′-3′)	Reference
ARCH915	Most archaea	Proteinase K	35	GTG CTC CCC CGC CAA TTC CT	Stahl and Amann 1991
AAA-FW-641	AOM-associated archaea, freshwater cluster	Proteinase K	60	GGT CCC AAG CCT ACC AGT	Schubert et al. 2011
AAA-FW-834			60	TGC GGT CGC ACC GCA CCT	Schubert et al. 2011
ANME-1-350	ANME-1	Proteinase K	40	AGT TTT CGC GCC TGATGC	Boetius et al. 2000
ANME-2-538	ANME-2	SDS	40	GGC TAC CAC TCG GGC CGC	Treude et al. 2005
EUB338 I-III	Most bacteria	Lysozyme	35	GCT GCC TCC CGT AGG AGT GCA GCC ACC CGT AGG TGT GCT GCC ACC CGT AGG TGT	Daims et al. 1999
Alf 968	alphaproteobacteria	Lysozyme	35	GGT AAG GTT CTG CGC GIT	Neef 1997
Ma450	Type II methanotrophs	SDS	20	ATC CAG GTA CCG TCA TTA TC	Eller and Frenzel 2001
Mgamma705	Type I methanotrophs	Lysozyme	20	CTG GTG TTC CTT CAG ATC	Eller and Frenzel 2001
Mgamma84			20	CCA CTC GTC AGC GCC CGA	Eller and Frenzel 2001
NON338	Negative control	Lysozyme	35	ACT CCT ACG GGA GGC AGC	Wallner et al. 1993

photosynthetic fractionation of 20‰ because several studies have observed lower fractionation (~ 17‰) in lakes (Kluijver et al. 2014; McCallister and del Giorgio 2008).

The fractionation factors (α) for aerobic CH_4 oxidation and anaerobic CH_4 oxidation were calculated after Hayes (1993) as:

$$\alpha = \left(\delta^{13}C_{Sub-CH_4} + 1000\right) / \left(\delta^{13}C_{Prod-CH_4} + 1000\right) \quad (2)$$

where the subscript "Sub-CH_4" refers to substrate CH_4 before microbial oxidation and "Prod-CH_4" indicates the product CH_4 left behind after microbial oxidation.

The proportional contribution of methanotrophic lipids to the PLFA was estimated using a binary isotopic mixing model below:

$$\delta^{13}C_{PLFA} = f \bullet \delta^{13}C_{methanotrophic} + (1 - f) \bullet \delta^{13}C_{Non-methanotrophic} \quad (3)$$

where "PLFA" is phospholipid fatty acids, f is the proportion of methanotrophic lipids, and (1 - f) is the proportion of non-methanotrophic lipids. We used a $\delta^{13}C$ value of −23‰ (as explained in Eq. 1) as the non-methanotrophic lipid endmember and a $\delta^{13}C$ value of −78‰ (as explained in Eq. 1) as the methanotrophic lipid endmember for the PLFA of type I and type II MOBs. As a much larger isotope fractionation (≥ 35‰) is associated with biomass synthesis by methanotrophic archaea during AOM (Blumenberg et al. 2004; Niemann and Elvert 2008), we used a $\delta^{13}C$ value of −97‰ (based on our measured 200 m methane $\delta^{13}C$ of −62‰ and assuming a fractionation of −35‰) as the methanotrophic lipid endmember for the PLFA of SRB.

Statistical analyses

We used STATISTICA (StatSoft) for the analyses. Statistical significance was tested at the 95% confidence level.

Quantification of bacterial and archaeal cells using CARD-FISH and 4′,6-diamidino-2-phenylindole

Five milliliter of lake water from 35 m, 50 m, 60 m, and 70 m (water-column depths) were fixed with formaldehyde (2%, v : v) overnight at 4°C in the dark. Samples were then filtered onto 0.2 μm polycarbonate GTTP filters (Millipore) and stored at −20°C until further processing. CARD-FISH

was performed using horseradish peroxidase (HRP)-labeled oligonucleotide probes to target specific microbial groups. Details of the probes (purchased from Biomers, Ulm, Germany) used for this study along with the respective formamide concentrations of hybridization buffer are provided in Table 1. Permeabilization with lysozyme (10 mg mL^{-1}) was done for 1 h at 37°C. With proteinase K (15 μg mL^{-1}) and sodium dodecyl sulfate (SDS; 0.5%, v : v) cell walls were permeabilized for 3 min and 10 min at room temperature, respectively. Filter pieces were then bleached with 0.1 mol L^{-1} HCl for 10 min at room temperature for inactivation of endogenic peroxidase activity. Hybridization with the respective probes and corresponding hybridization buffers was completed for 2.5 h at 46°C. Probes were used in a 1 : 1 mix where the same group was targeted, that is, AOM-associated archaea (AAA-FW) (Schubert et al. 2011) and type I methanotrophs (Mgamma) (Eller and Frenzel 2001). Probes were amplified with the tyramide Oregon Green 488 (1 μl mL^{-1}) for 30 min at 37°C. Finally, filters were counterstained with 4′,6-diamidino-2-phenylindole (DAPI) (1 μl mL^{-1}) and dried before they were embedded (4 : 1, Citifluor : Vectashield) and mounted onto glass slides. Cells were enumerated with an epifluorescence microscope (Zeiss Axioskop 2) by counting 20 independent fields of view. On average, 200 cells per field of view were counted with DAPI and probes EUB338 I–III (Daims et al. 1999). If signals were detected, averages of 10 cells per field of view were counted for all other probes used (Table 1). The percentages of the probe signals were calculated based on total cell numbers, which were counted with DAPI. Background signal (negative control) based on the probe NON338 (Wallner et al. 1993) was negligible in all the samples.

Results

Temperature, dissolved oxygen, and reduced species

Dissolved O_2 concentration in the surface waters ($\leq$ 13 m) was $\sim$ 237 μmol L^{-1} (Fig. 2a). The depth profile of dissolved O_2 shows two oxyclines; one at 13−26 m where the concentration decreased slightly and steadily from 237 μmol L^{-1} to 210 μmol L^{-1}, and the other at 26–31 m showing a sharp decrease in oxygen concentration from 210 μmol L^{-1} to 30 μmol L^{-1} (Fig. 2a). The dissolved O_2 level remained fairly stable at 30 μmol L^{-1} until 48 m where the value dropped to 1 μmol L^{-1} (Fig. 2a). Concentrations below the sensor detection limit of 0.02 μmol L^{-1} (referred to as "anoxic" throughout the rest of the article) were observed below 52 m water depth (Fig. 2a). The temperature profile exhibited two thermoclines, decreasing gradually from 25.5°C to 23.9°C at 1–25 m depth layer and a slight but sharp decline from 23.9°C to 23.4°C at $\sim$ 26–32 m (Fig. 2a). The temperature was around 23°C in the deep waters (below 50 m) and showed an increasing trend with depth after 80 m (Fig. 2a). Concentrations of the reduced species showed a pronounced chemocline in the deep anoxic waters (Fig. 2b). The deep source of the reduced species was reflected in the increase with depth of the concentration of NH_4^+ from 18 μmol L^{-1} to 434 μmol L^{-1}, of S(-II) from 9 μmol L^{-1} to 196 μmol L^{-1}, and of NO_2^- from 0.1 μmol L^{-1} to 38.0 μmol L^{-1} within the anoxic depths 60–90 m (Fig. 2b). The values of ammonium and sulfide were low within the oxic-anoxic transition zone (31–52 m) and negligible in the oxic region of the lake (Fig. 2b).

Stable carbon and nitrogen isotopic composition of SPM

The SPM from the lake at 60–90 m showed relatively more ^{13}C-depletion (δ^{13}C, −29.8‰ to −28.1‰) than the SPM in the region of 5–55 m (δ^{13}C, −25.4‰ to −21.9‰) and in the deeper layers at 140–200 m (δ^{13}C, −24.4‰ to −24.1‰; Fig. 3). The SPM in the surface 5–10 m was more ^{15}N-depleted (δ^{15}N, 0.1–0.9‰) than the other depth regions in the lake (Fig. 3). The most ^{15}N-enriched SPM (δ^{15}N of 7.4–9.6‰) was observed at 50–70 m, and interestingly, coincided with the minimum in the δ^{13}C-profile of SPM (Fig. 3).

Concentration and isotopic composition of CH_4 and DIC

Between 50 m and 200 m, CH_4 and DIC concentrations increased from 0.02 mmol L^{-1} to 2.9 mmol L^{-1} and from 11.5 mmol L^{-1} to 51 mmol L^{-1}, respectively (Fig. 4a,b). Above 50 m water depth, CH_4 and DIC concentrations in the lake varied only slightly and were $\sim$ 0.01 mmol L^{-1} and $\sim$ 10 mmol L^{-1}, respectively (Fig. 4a,b). The δ^{13}C values of CH_4 in the deep water at 140–200 m were $\sim$ −62‰ and were slightly but significantly (*t*-test, $p < 0.05$) more ^{13}C-depleted than the values at 50–90 m (−60‰ to −56‰; Fig. 4a). In the surface waters, CH_4 was more ^{13}C-enriched with a δ^{13}C–CH_4 of −57‰ at 50 m and −30‰ at 5 m (Fig. 4a). The δ^{13}C of DIC was ^{13}C-depleted in the anoxic waters (e.g., 1.6‰ at 200 m) relative to the surface waters (e.g., 4.5‰ at 5 m; Fig. 4b).

Fatty acids

The fatty acid C16:1ω5 from the SPM had a concentration of $\leq$ 0.03 μg L^{-1} and exhibited more ^{13}C-depletion (δ^{13}C of −50.6‰ to −44.8‰) in the deep anoxic waters ($\geq$ 52 m) than in the surface waters (δ^{13}C of −32.8‰ to −29.5‰; Table 2, Fig. 5a). Similarly, the fatty acid C16:1ω7 also showed more ^{13}C-depletion in the anoxic waters (δ^{13}C of −42.6‰ to −38.9‰), one exception being the δ^{13}C of −33.0‰ seen at 140 m (Fig. 5b). However, C18:1ω7 fatty acid from the SPM, with a concentration of $\leq$ 24.1 μg L^{-1}, was more ^{13}C-depleted (−43.7‰ to −40.5‰) in the oxic surface waters than in the deep anoxic waters (−35.3‰ to −28.9‰; Fig. 5c). The fatty acid *anteiso*-methyl-C15:0 (*ai*-C15:0) from the SPM had concentration of $\leq$ 0.9 μg L^{-1} and was more ^{13}C-depleted (δ^{13}C of −45.0‰ to −38.2‰) in the deep anoxic waters than in the surface waters (δ^{13}C of −32.8‰ to −26.6‰) of the lake (Table 2, Fig. 5d).

GDGTs and archaeol

Archaeol in the SPM from the anoxic waters had a concentration of 0.9–7.8 ng L^{-1}, with the highest concentration (7.2–7.8 ng L^{-1}) observed at 70–80 m in the lake (Fig. 6a).

Table 2. Concentrations and stable carbon isotope distributions of individual fatty acids within SPM from the water column of Lake Kivu. Fatty acids were analyzed as FAMES. Precision of $\delta^{13}C$ values, based on duplicate analyses, was $\leq 1‰$, and precision of the concentration, based on multiple analyses of external standard, was $\leq 4\%$.

Depth (m)	5		10		35		50		62		70		100		140	
Volume (L)	41		41		77		72		126		108		135		135	
Fatty acid	$\times 10^2$ ng L^{-1}	$\delta^{13}C$ (‰)	$\times 10^2$ ng L^{-1}	$\delta^{13}C$ (‰)	ng L^{-1}	$\delta^{13}C$ (‰)	ng L^{-1}	$\delta^{13}C$ (‰)	ng L^{-1}	$\delta^{13}C$ (‰)	ng L^{-1}	$\delta^{13}C$ (‰)	ng L^{-1}	$\delta^{13}C$ (‰)	ng L^{-1}	$\delta^{13}C$ (‰)
C14:0	39.5	nd	30.6	nd	315.2	nd	53.9	nd	nd	nd	14.4	nd	nd	nd	0.0	nd
C:15:0	2.1	nd	2.3	nd	46.7	−26.9	11.2	−24.8	nd	nd	19.3	−29.1	9.5	−40.4	1.6	−36.8
ai-C:15:0	0.8	nd	0.9	nd	24.8	−32.8	5.3	−26.6	0.8	nd	34.7	−38.2	22.0	−45.0	4.8	−43.9
C16:1ω7	41.6	nd	35.3	nd	193.4	nd	37.6	nd	5.0	−38.9	66.2	−40.1	17.5	−42.6	2.7	−33.0
C16:1ω5	nd	−32.4	nd	−32.8	14.9	−32.5	4.5	−29.5	0.4	−44.8	26.3	−49.4	6.0	−50.6	nd	−46.0
C16:0	272.4	−27.7	263.4	−31.7	1993.3	−36.6	236.6	−26.0	19.2	−36.7	232.8	−35.9	132.1	−40.4	37.4	−30.4
C18:2	nd	nd	213.6	−30.5	454.6	−32.9	89.9	−27.4	12.6	−29.1	91.1	−28.3	70.1	−37.5	17.3	−25.7
C18:1ω9	114.1	−43.3	125.3	−32.4	891.3	−39.2	108.1	−32.2	11.9	−36.3	131.5	−34.3	81.4	−40.9	22.3	−33.2
C18:1ω7	24.3	−43.7	nd	−41.9	157.5	−40.5	42.3	−28.9	13.0	−34.3	47.3	−35.3	22.6	nd	7.1	nd
C18:0	21.3	−32.1	20.7	nd	189.2	−32.6	27.8	nd	nd	−45.2	52.1	nd	37.2	−40.4	12.2	−32.5
C20:0	nd	nd	2.0	nd	11.8	nd	nd	nd	nd	nd	11.1	nd	8.5	−36.9	10.9	−25.6
C22:0	6.2	−34.9	5.8	nd	30.4	−34.7	1.3	nd	nd	nd	nd	nd	7.3	−42.2	3.4	−31.1
C24:0	1.6	−37.5	1.5	nd	16.4	nd	nd	nd	nd	nd	nd	nd	2.9	nd	2.2	−27.2

nd = not determined or lost during processing of samples in the field or lab.

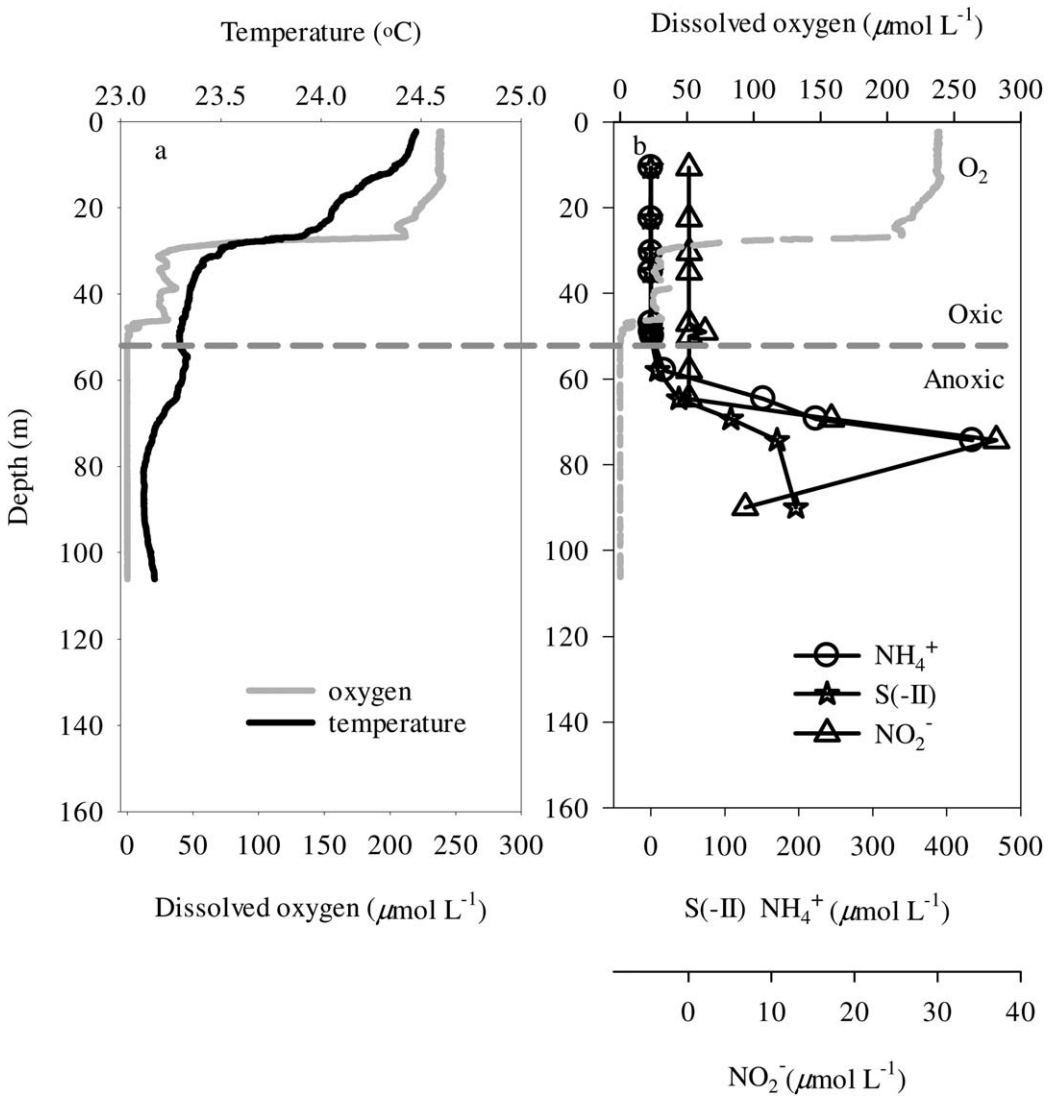

Fig. 2. Depth profiles of (a) dissolved oxygen and temperature in the water column showing two oxyclines and thermoclines at ~13-25 m and 25–32 m; anoxia (dissolved oxygen concentration below 0.02 μmol L^{-1}) is established below 52 m (Winkler concentrations are 237.5 ± 6.3 μmol L^{-1} at 2 m depth) and (b) the vertical distributions of ammonium (NH_4^+), total sulfide (S(-II)) and nitrite (NO_2^-) in the water column; a pronounced chemocline is observed between 60 m and 80 m. As is the case for all subsequent plots, the horizontal dashed line is the oxic-anoxic transition at 52 m depth.

The $\delta^{13}C$ of archaeol was −39.8‰ to −26.2‰, with the exception of a more ^{13}C-depleted archaeol (−52.1‰) value at 80 m (Fig. 6a). The concentration of GDGT-0 in the SPM was 0.1–4.3 ng L^{-1} and GDGT-IV (crenarchaeol) concentration was 0.2–38.3 ng L^{-1} (Fig. 6b). The ratios GDGT-0 : GDGT-IV and GDGT-0 : IsoGDGTs were invariant in the oxic surface waters, being ~ 0.10 and 0.06 units, respectively (Fig. 6b) but increased with depth in the anoxic waters (55–200 m) from 0.10 to 6.9 and 0.06 to 0.64, respectively (Fig. 6b).

Phytol, brassicasterol, dinosterol, and cholesterol

Concentrations of phytol, brassicasterol, dinosterol, and cholesterol were higher in the oxic surface waters than in the anoxic region of the lake (Fig. 7b-e), and ranged from 6-916 ng L^{-1}, 3–83 ng L^{-1}, 7–147 ng L^{-1} and 8–257 ng L^{-1}, respectively. $\delta^{13}C$ values of phytol, brassicasterol, dinosterol, and cholesterol within the SPM from the lake ranged from −42.3‰ to −31.8‰, −43.8‰ to −29.9‰, −29.1‰ to −19.1‰, and −41.5‰ to −20.3‰, respectively (Fig. 7b-e).

Depth distribution of bacteria and archaea in the water column of Lake Kivu

Bacteria dominated the prokaryotic community in the lake with cell numbers ranging from 4.6×10^5 cells mL^{-1} at 70 m to 8.0×10^5 cells mL^{-1} at 50 m, representing 57–81% of the total DAPI stained cells (6.8×10^5–8.2×10^6 cells mL^{-1}; Fig. 8a,b). Archaeal cell numbers were consistently lower than those of bacteria in the lake and ranged from 0.1×10^5 cells

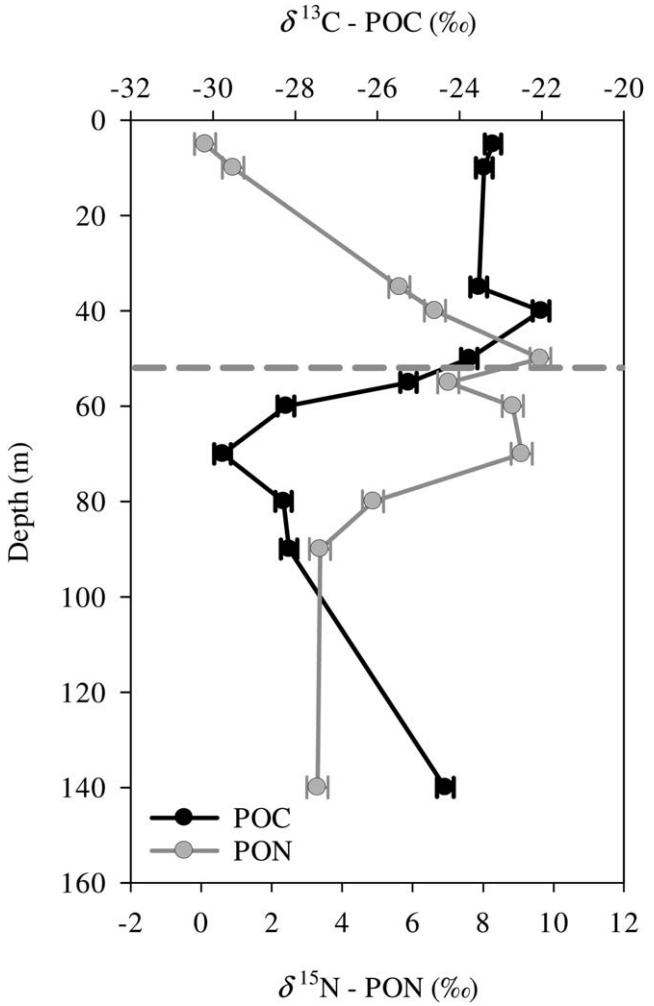

Fig. 3. Vertical profiles of the stable carbon and nitrogen isotopic compositions of SPM.

mL^{-1} at 60 m to 1.5×10^5 cells mL^{-1} at 35 m, representing 1–12% of the total DAPI stained cells (Fig 8a,b). Alphaproteobacteria were less abundant in the lake, with cell numbers < 3% of the total DAPI stained cells. The cell numbers of type I MOB were 0.13×10^5 cells mL^{-1} (1.3% of DAPI stained cells), 0.05×10^5 cells mL^{-1} (0.6% of DAPI stained cells), and 0.04×10^5 cells mL^{-1} (0.6% of DAPI stained cells) at 50 m, 60 m, and 70 m, respectively (Fig. 8a,b). Type II MOB were less abundant than type I MOB with cell numbers of 0.03×10^5 cells mL^{-1} (0.3% of DAPI stained cells) and 0.01×10^5 cells mL^{-1} (0.2% of DAPI stained cells) at 50 m and 70 m, respectively (Fig. 8a,b). Type I MOB cells were not observed at 35 m, and type II MOB cells were not observed at either 35 m or 60 m in the lake (Fig. 8a). ANME-1 and ANME-2 (probes ANME-1-350 (Boetius et al. 2000) and ANME-2-538 (Treude et al. 2005)) and AOM-associated archaea (probes AAA-FW-641 and AAA-FW-834; Schubert et al. 2011) were not detected in the lake (Fig. 8a).

Discussion

Bulk CH_4 isotopic insights into microbial CH_4 oxidation

The observed ^{13}C-enrichment of CH_4 between 52 m and 90 m (relative to CH_4 from deeper depths, 140–200 m; Fig. 4a) is due to preferential microbial oxidation of lighter CH_4 ($^{12}CH_4$) leading to ^{13}C-enrichment of the residual CH_4 pool. This implies that anaerobic CH_4 oxidation occurs within this anoxic region of the lake. However, the slight offset in $\delta^{13}C$ of CH_4 between 140–200 m and 52–90 m ($\Delta\delta^{13}C$ of 2–6‰; Fig. 4a), corresponding to an anaerobic methane oxidation isotope fractionation factor (α) of 1.002–1.006 (Eq. 2), indicates that a small amount of CH_4 is consumed through anaerobic CH_4 oxidation in the lake. In contrast, the large offset in $\delta^{13}C$ of CH_4 between the anoxic region (52–90 m) and the oxic region (5–35 m; $\Delta\delta^{13}C$ of 21–36‰), corresponding to an aerobic methane oxidation α of 1.022–1.038, indicates intense aerobic microbial CH_4 consumption in the lake, which is corroborated by the drastic decrease in CH_4 concentration in the oxic region (Fig. 4a).

Our observation is consistent with other studies that observed that aerobic methane oxidation was the main sink of methane in Lake Kivu (Pasche et al. 2009). Pasche et al. (2009) noted a relatively higher total oxygen flux (57 g C m^{-2} yr^{-1}) compared to the methane upward flux (35 g C m^{-2} yr^{-1}) in the oxic surface waters (0–60 m), hence, aerobic methane oxidation may be primarily responsible for methane removal in Lake Kivu.

The observed fractionation factor for aerobic CH_4 oxidation in Lake Kivu is consistent with the reported value ($\alpha = 1.037$) in the water column of Lake Mekkojärvi, Southern Finland (Kankaala et al. 2007). The aerobic CH_4 oxidation α in Lake Kivu is, however, larger than the α of 1.005 observed in Lake Matano (Indonesia) (Crowe et al. 2011). The fractionation factor ($\alpha = 1.002 - 1.006$) for anaerobic CH_4 oxidation in Lake Kivu is consistent with reported values ($\alpha = 1.005 - 1.008$) in other anoxic systems (Whiticar 1999).

Preferential oxidation of $^{12}CH_4$ should lead to the production of ^{12}C-enriched CO_2 (Templeton et al. 2006). However, this was not observed in Lake Kivu (Fig. 4b) most likely because of the enormous volume of CO_2 in the lake (300 km^3; Schmid et al. 2005) masking the isotopic effect of the CO_2 produced from CH_4 oxidation (estimated at 31–33 g C m^{-2} yr^{-1}; Jannasch 1975; Pasche et al. 2011). Also, other biochemical processes such as photosynthesis in the surface waters (which result in ^{12}C-depletion of residual CO_2 or DIC) and respiration in the deep waters (which result in ^{12}C-enrichment of residual CO_2 or DIC) could be more important than CH_4 oxidation in modulating the isotopic signature of the CO_2 or DIC in the lake.

Contribution of methane carbon to the Lake Kivu food web

CH_4 is a significant carbon reservoir in Lake Kivu, therefore, we used biomarkers to evaluate whether CH_4 was an

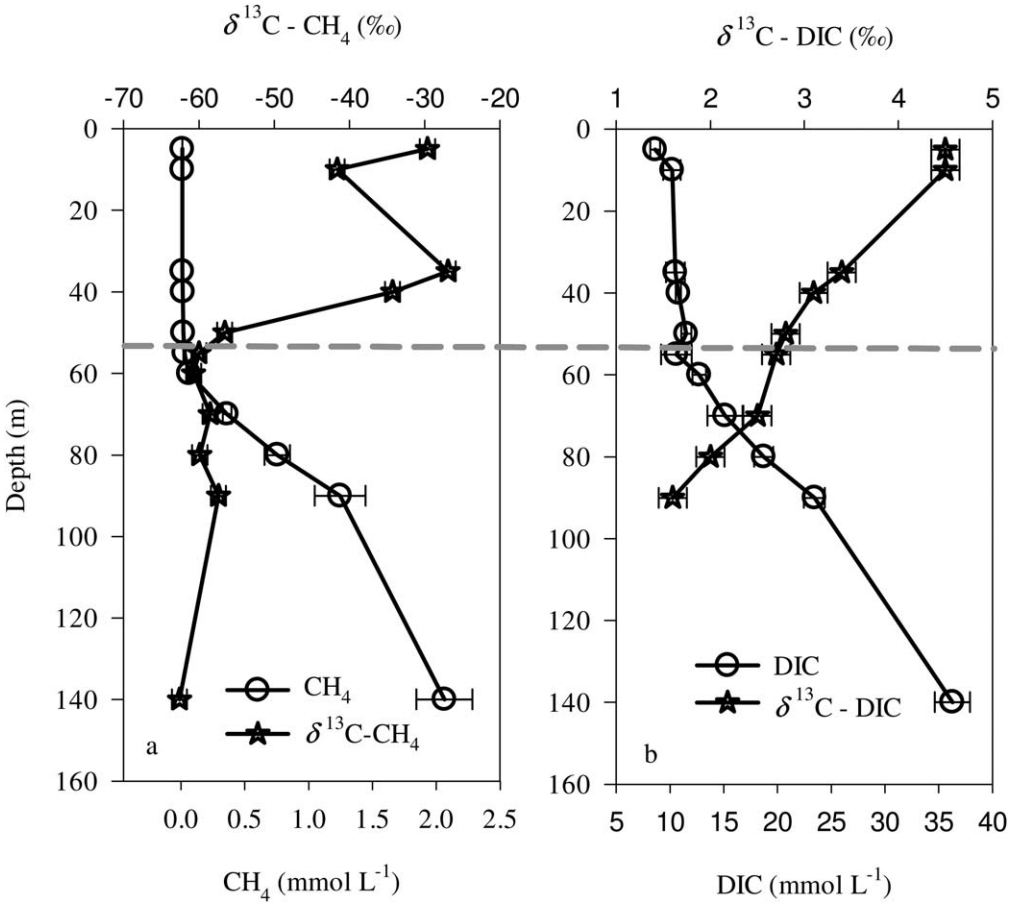

Fig. 4. Vertical profiles of the concentration and stable carbon isotopic compositions of (a) methane and (b) DIC in the water column of Lake Kivu.

important source of carbon and energy for the lake food web. Consumption of CH_4 by methanotrophic bacteria during CH_4 oxidation converts CH_4 carbon into microbial biomass. Subsequently, this methanotrophic biomass can serve as a carbon and energy source for heterotrophic organisms via zooplankton grazing on methanotrophic bacteria, or the use of inorganic carbon from mineralized methanotrophic biomass by autotrophs. In Lake Kivu, the $\delta^{13}C$ values of biomarkers for phytoplankton including cyanobacteria (phytol; $\delta^{13}C$ of $-42.3‰$ to $-31.8‰$), diatoms (brassicaterol; $\delta^{13}C$ of $-43.8‰$ to $-29.9‰$), dinoflagellates (dinosterol; $\delta^{13}C$ $-29.1‰$ to $-19.1‰$), and a biomarker for zooplankton and other heterotrophs (cholesterol; $\delta^{13}C$ of $-41.5‰$ to $-20.3‰$; Fig. 7) indicate that eukaryotic phototrophs and heterotrophic grazers in the lake derive some of their carbon and energy from CH_4. Using a binary isotopic mixing model (Eq. 1), the contribution of CH_4 carbon to phytol, brassicasterol, and cholesterol within SPM in the lake was estimated at 16–35%, 13–38%, and $\leq 34\%$, respectively. The autotrophic plankton community in Lake Kivu is dominated by cyanobacteria, mainly *Synechococus sp*. and *Planktolyngbya limnetica*, and diatoms, mainly *Nitzschia bacata* and *Fragilaria Danica* (Sarmento et al. 2012). Other phytoplankton groups such as dinoflagellates and cryptophytes are also present in the lake. In their detailed study of the vertical distribution of phytoplankton groups in the main basin of Lake Kivu off Kibuye, Sarmento et al. (2012) reported that diatoms were the dominant phytoplankton in the lake during deep mixing conditions (where the upper mixed layer is deeper than 50 m) in the dry season (June–September), whereas diazotrophic cyanobacteria and picocyanobacteria are dominant during the rainy season (October–May). The use of methane-derived carbon by photoautotrophs in Lake Kivu is interesting. However, both the mineralization of methanotroph-derived organic matter (e.g., from dead aerobic methanotrophic bacteria and zooplankton supported by methanotrophic bacteria and archaea) and the oxidation of methane to CO_2 could generate methane-derived dissolved carbon dioxide that could be utilized by the autotrophic plankton during photosynthesis. This agrees with the assertion by Pasche et al.

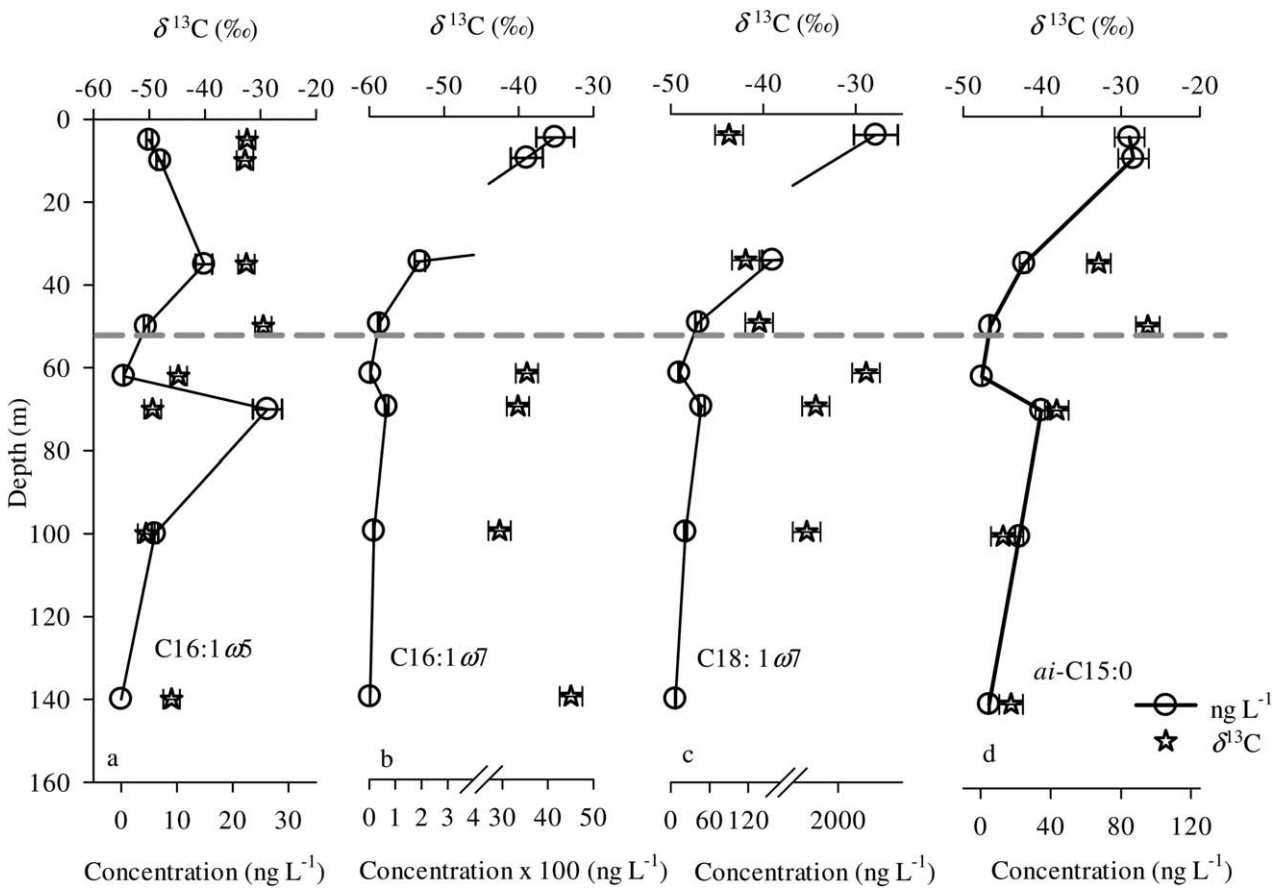

Fig. 5. Vertical distributions of the concentrations and stable carbon isotopic compositions of the PLFA (a) C16:1ω5, (b) C16:1ω7, (c) C18:1ω7, and (d) *anteiso*-methyl-C15:0. C16:1ω5 and *ai*-C15:0 fatty acids were more ^{13}C-depleted in the deep waters below 52 m whereas C18:1ω7 showed more ^{13}C-depletion in the oxic surface waters.

(2009) that uptake of methane by picoplankton could be a sink of methane in the surface oxic layers of the lake and is consistent with the observation by Llirós et al. (2012) that mineralization of organic matter coupled to oxidation of reduced species including methane can result in a rapid decrease in oxygen concentrations in the lower mixolimnion (25–30 m to $\sim$ 65 m) after thermal stratification begins in October–November. Also, Morana et al. (2014) observed that methane contributes significantly to carbon fixation in the oxic-anoxic interface in Lake Kivu. The heterotrophic community in Lake Kivu could derive some of their carbon from methane through grazing on methanotrophic archaea and bacteria, as well as methane-supported phototrophs. For instance, Descy et al. (2012) noted that methanotrophic archaea and bacteria likely contribute to planktonic crustacean production in Lake Kivu. Support of the food web by CH_4 carbon in Lake Kivu is consistent with previous studies in other aquatic systems. Werne et al. (2002) used the isotopic composition of biomarkers to trace methane-derived carbon through microbes into heterotrophic ciliates. Also, in their study of zooplankton carbon isotope signatures in three lakes in Sweden (Illersjön, Marn, and Lillsjön), Bastviken et al. (2003) reported that 5–15% of zooplankton production was supported by methanotrophic biomass. In Lake Kivu, it was interesting to observe that below the chemocline in the anoxic waters (70–80 m depth), the δ^{13}C values of the biomarkers of phototrophs and heterotrophs were ^{13}C-depleted relative to shallower oxic waters (Fig. 7). The ^{13}C-depletion of heterotrophic organisms at this depth range could be from anaerobic methane-oxidizing archaea, SRB involved in AOM and/or their heterotrophic grazers. Also, chemoautotrophic and chemoheterotrophic bacteria or archaea (Llirós et al. 2012) supported by methane or methane-derived CO_2 and their heterotrophic grazers could contribute to the observed ^{13}C-depletion of heterotrophic organisms observed at this depth region. The ^{13}C-depletion of phototrophs at this depth suggests deeper anoxygenic photosynthetic activity. The anoxygenic photoautotrophs, green sulfur bacteria (GSB), are commonly found in the upper anoxic layers of the lake (Llirós et al. 2012). Although a small amount of light ($\leq$ 1% of the light intensity at the surface) potentially reaches this depth region below the euphotic zone, the

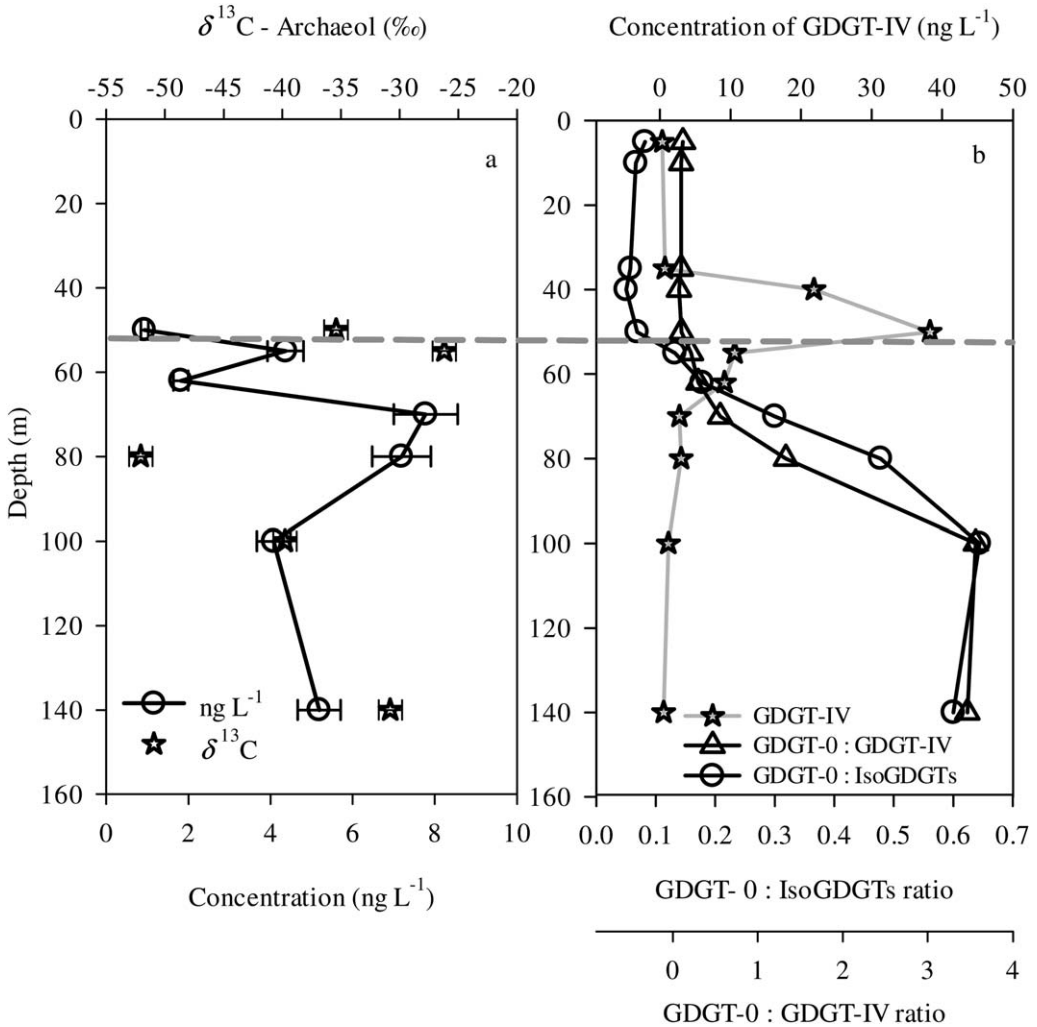

Fig. 6. Vertical distributions of (a) the concentration and stable carbon isotopic composition of archaeol and (b) the concentration of GDGT-IV, and the values of the ratios of GDGT-0 to isoGDGTs and GDGT-0 to GDGT-IV in the water column of Lake Kivu. Values < 1 of the ratio of GDGT-0 to GDGT-IV and GDGT-0 to isoGDGT (Fig. 6b) indicate relatively lesser contributions from methanogenic archaeal lipids compared to lipids from crenarchaeota and other archaea groups throughout the water column. The increasing values of GDGT-0:isoGDGTs and GDGT-0:GDGT-IV with depth in the anoxic region shows the increasing contribution from methanogens to the archaeal biomass.

obligate anaerobic bacteria GSB are known to be able to photosynthesize under extreme low-light conditions using hydrogen sulfide, hydrogen, or Fe (II) as an electron donor (Llirós et al. 2012). Carbon fixation by GSB using methane-derived CO_2 could explain the ^{13}C-depleted biomarkers of phototrophs observed at this depth. Also, some minimal carbon fixation by phototrophs such as cyanobacteria could contribute to the observed ^{13}C-depletion of the biomarkers of phototrophs at this depth region.

Methanotrophic communities mediating methane oxidation in the oxic ozone

Molecular isotopic evidence of aerobic CH_4 consumption by MOB comes from the ^{13}C-depletion of the fatty acid C18:1ω7 seen in the oxic surface waters but not in the deep anoxic waters of the lake (Fig. 5c). The fatty acids C18:1ω8 and C18:1ω7 are diagnostic of type II MOB (Hanson and Hanson 1996; Bodelier et al. 2009). Therefore, the higher concentrations coupled to ^{13}C-depletion of C18:1ω7 fatty acids in the surface waters (Fig. 5c) indicate that type II MOB are consuming CH_4 in the oxic surface waters. In contrast, C16:1ω5 (and C16: 1ω7) fatty acids, which are diagnostic of type I MOB (Kankaala et al. 2007; Bodelier et al. 2009), were not ^{13}C-depleted in the surface waters (Fig. 5a,b), implying that type I MOB were not involved in CH_4 oxidation in the surface waters. In a related study in Lake Kivu, Pasche et al. (2011) detected the methane monooxygenase (*pmoA*) gene (a molecular marker for aerobic methanotrophs) in particles at 40 m and 60 m (both oxic depths in that study) and observed that the *pmoA* sequences were closely related to *Methylococcus capsulatus* (type X MOB). It should be noted that while this is not consistent with our

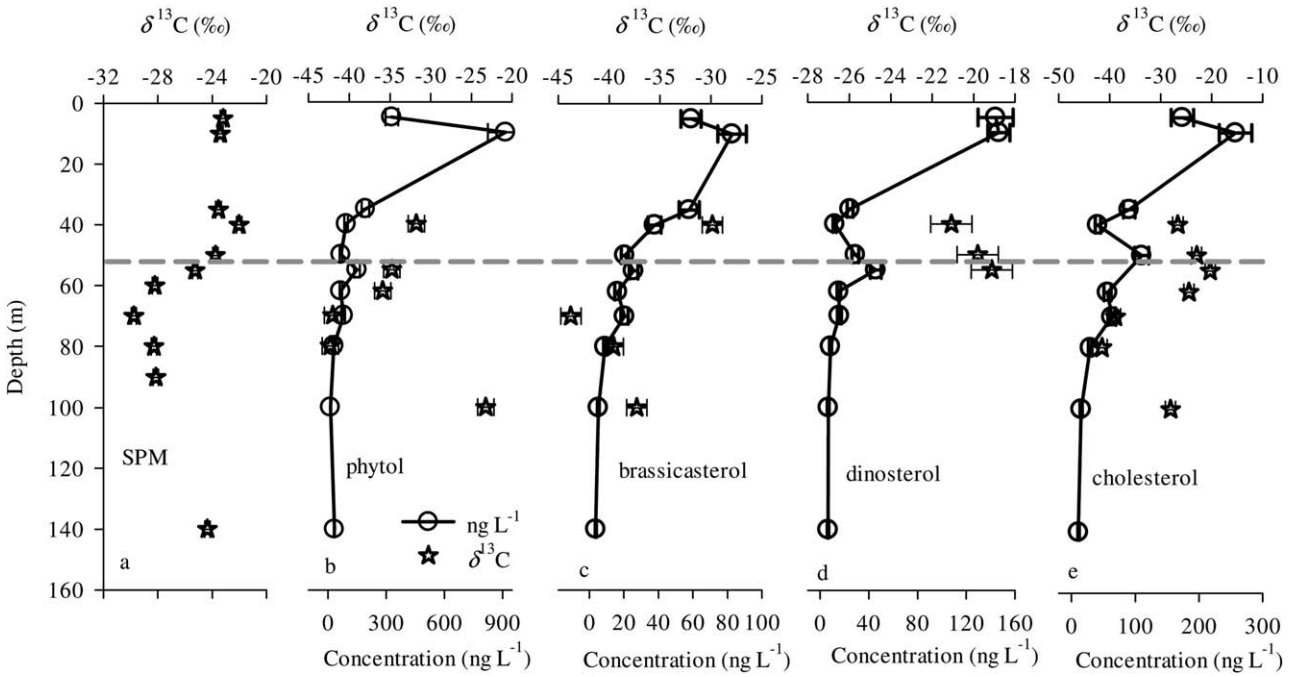

Fig. 7. Vertical distribution of the concentration and stable carbon isotopic composition of (b) phytol, (c) brassicasterol, (d) dinosterol, and (e) cholesterol in the water column of Lake Kivu. The isotopic composition of (a) SPM has been included here for comparison.

observation that type II MOB is mainly responsible for aerobic methane oxidation in Lake Kivu, Pasche et al. (2011) also indicated that the primer set used in that study had a potential bias toward type X MOB and that different and/or diverse communities could have been involved in aerobic methane oxidation.

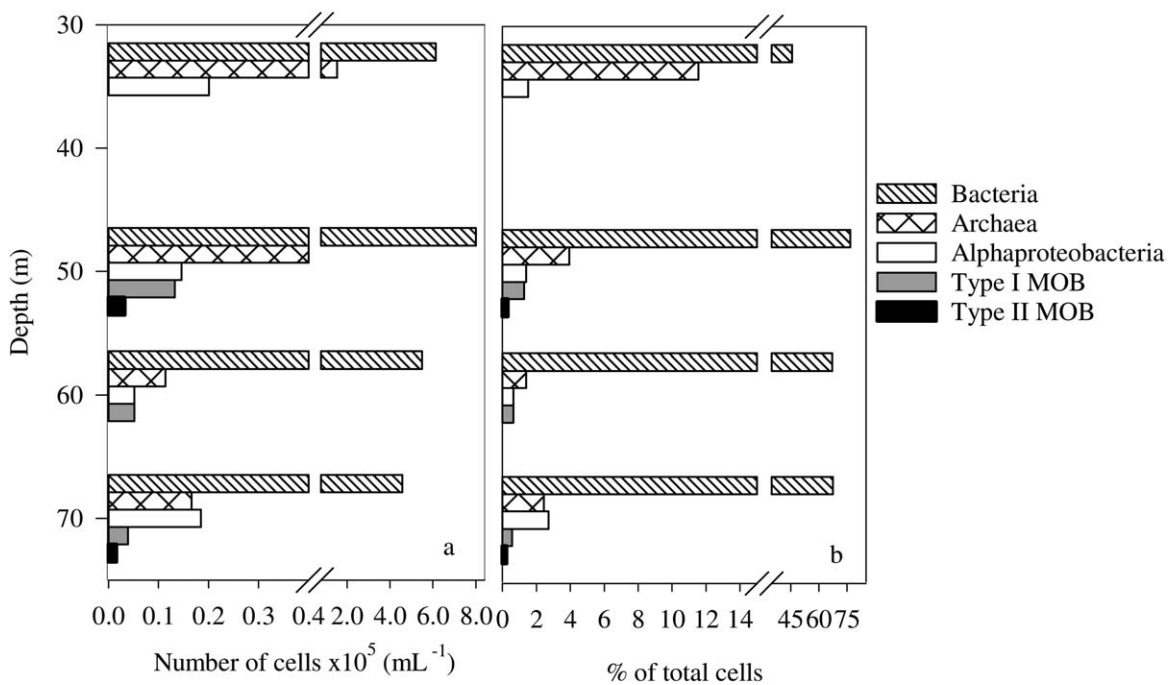

Fig. 8. Distributions of the (a) cell numbers, and (b) relative percentages of bacteria, archaea, alphaproteobacteria, type I MOB, and type II MOB in the water column of Lake Kivu. Positive hybridization with ANME specific probes was not observed at these water depths in the lake.

The apparent habitat specialization of MOB in Lake Kivu as observed in this study, where type II MOB are active in the nutrient-limited oxic surface waters and type I MOB are active within the methane and nutrient-rich deep-water region with ≤ 20 nmol L^{-1} oxygen ("anoxic" region) is interesting and could be linked to the chemical species regime in the lake. Tavormina et al. (2013) have also reported increased abundance of type I MOB at the upper and lower horizons of oxygen minimum zones off of Costa Rica. Previous studies have reported the predominance of type II MOB under nutrient-limiting (nitrogen or copper-depleted) conditions and the predominance of type I MOB in favorable growth (nitrogen and copper-rich) conditions (Amaral and Knowles 1995). In small, eutrophic Lake Rotsee in Switzerland, type I MOB predominated in the aerobic oxidation of CH_4 (Schubert et al. 2010) most likely due to nutrient (e.g., nitrogen; Schubert et al. 2010) rich conditions in the lake. Similarly, type I MOB is the predominant MOB in nutrient-rich Lake Constance (Rahalkar et al. 2009). In contrast, the predominance of type II MOB in the aerobic oxidation of CH_4 in Lake Kivu could be due to the oligotrophic, nutrient-poor (low levels of nitrogen and copper) conditions of the oxic surface waters (Lliros et al. 2010; Julius 2011).

CH_4 oxidation by type I MOB in the deep waters

Fatty acids C16:1ω8, C16:1ω7, and C16:1ω5 are diagnostic of type I MOB as noted earlier and are characteristic of the genera *Methylomonas* (C16:1ω8), *Methylobacter* (C16:1ω7 and C16:1ω5), *Methylococcus* (C16:1ω7), and *Methylomicrobium* (C16:1ω5 and C16:1ω7) (Hanson and Hanson 1996; Kankaala et al. 2007; Bodelier et al. 2009). The presence of C16:1ω5 and C16:1ω7, and their considerable ^{13}C-depletion in the deep-water region below 52 m (Figs. 5a,b), suggest the involvement of type I MOB in CH_4 oxidation in the anoxic deep-water region (with ≤ 20 nmol L^{-1} oxygen concentration) of the lake. This is corroborated by the presence of type I MOB throughout the sampled deep-water depths as determined from CARD-FISH analysis (Fig. 8a).

Alternatively, the ^{13}C-depleted fatty acids from SPM observed in the deep waters of the lake could be from sinking inactive or dead bacterial biomass of type I MOB from the oxic overlying surface waters. However, the same fatty acid species in surface-water SPM were not as ^{13}C-depleted as in the deep waters, which should have been the case if the deep-water fatty acids had originated from the surface waters. Also, because of the consistent ^{13}C depletion of these fatty acids at multiple depths in the deep-water region (which would not be the case for just an episodic sinking of SPM from the surface region), it is unlikely that the observed ^{13}C-depleted C16:1ω5 and C16:1ω7 originated from the surface waters.

The exact physical or biochemical pathway or mechanism that is driving the aerobic methane oxidation in the deep waters is not known. It is possible that the type I MOB are utilizing very low O_2 concentrations ($\leq$ 20 nmol L^{-1}) for methane oxidation, or that there is a temporal input of dissolved oxygen from the subaquatic springs feeding the anoxic regions of the lake. Coupling of the aerobic methane oxidation with deep-water photosynthetic activity or the reduction of oxidized nutrients or metals are also possible.

Presence of SRB and potential coupling with ANME in anaerobic methane oxidation

The pathway of anaerobic methane oxidation can be examined in the context of the vertical distribution of potential electron acceptors in the anoxic region. In Lake Kivu, the reduction of sulfate to sulfide is revealed by the opposite depth gradients of SO_4^{2-} and S(-II) within 60–90 m in the anoxic region (Fig. 2b; Pasche et al. 2009). This observation, coupled to the inverse depth profiles of methane and sulfate within 60–90 m suggest that anaerobic methane oxidation via sulfate reduction occurs within this anoxic region in the lake (Pasche et al. 2009, 2011). By comparing the total sulfate flux (1 ± 0.5 g C m^{-2} yr^{-1}) and methane upward flux (35 ± 0.5 g C m^{-2} yr^{-1}), Pasche et al. (2009) noted that a maximum of only 3% of the methane could be anaerobically oxidized via sulfate reduction. The fluxes of nitrate, nitrite, and oxidized iron or manganese are too low, and likely play a negligible role in anaerobic methane oxidation in Lake Kivu (Pasche et al. 2011; Llirós et al. 2012).

A syntrophic cooperation between SRB and ANME oxidize CH_4 under anoxic conditions through electron transfer from the CH_4 to sulfate (Boetius et al. 2000). However, in a recent study, Milucka et al. (2012) observed that ANME alone (without SRB partnership) may be able to carry out AOM through dissimilatory reduction of sulfate to zero-valent sulfur.

The fatty acids *ai*-and *i*-C15:0 and -C17:0 are diagnostic of SRB (Wakeham et al. 1997; Pancost et al. 2000). Kohring et al. (1994) reported that *ai*-C15:0 was a major constituent of the membrane lipids of the SRBs *Desulfosarcina variabilis* and *Desulfococcus multivorans*. Although the fatty acids *ai*- and *i*-C15:0 and -C17:0 have also been found in some iron and manganese oxidizers, the observed ^{13}C-depletion of the fatty acid *ai*-C15:0 (δ^{13}C of -45.0‰ to -38.2‰; Fig. 5d) in anoxic waters overlapping the sulfate reduction zone suggests that this fatty acid most likely originated from SRB involved in AOM (rather than Mn or Fe-reducers with a negligible role in AOM) in the lake. This observation is consistent with Pasche et al. (2011) who used DGGE of PCR-amplified 16S rRNA gene fragments and found a deltaproteobacteria sequence with high similarity to the SRB *Desulfocapsa* within the sulfate reducing zone (60–90 m). Also, Schmitz (2011), using DGGE analysis, found deltaproteobacteria in the anoxic region (50–100 m) of the lake. In addition to the very low fluxes of iron and manganese, the Mn^{2+} depth profile in the lake (cf. Fig. 2a; Pasche et al. 2011) does not show coupling with AOM in the lake. Consequently, *ai*-C15:0 fatty acids from Mn reducing bacteria would not be

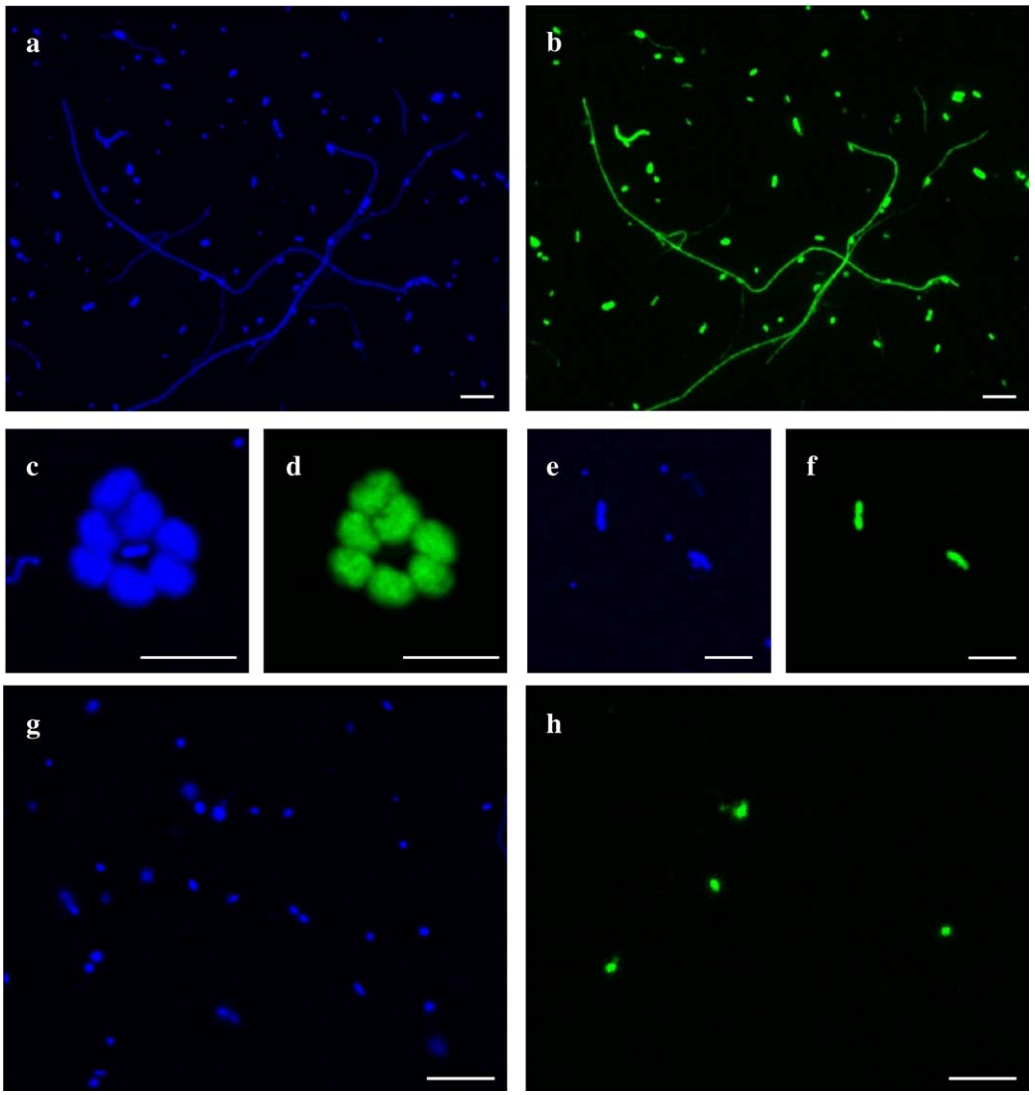

Fig. 9. Cells of microbial communities from the water column of Lake Kivu showing: (a,b) DAPI staining from 50 m and the corresponding CARD-FISH image for bacterial cells (probes EUB338 I-II) at 50 m. (c,d) DAPI staining from 70 m and the corresponding CARD-FISH image of type I MOB (probes Mgamma705 + 84) from 70 m. (e, f) DAPI staining and corresponding CARD-FISH image for type II MOB from 70 m (probe Ma450). (g, h) DAPI staining and corresponding archaeal signals from 50 m water depth (probe ARCH915). Note all scale bars = 5 μm. All images show confocal scanning micrographs.

^{13}C-depleted in contrast to *ai*-C15:0 fatty acids from SRB involved in AOM.

Our observations in Lake Kivu are consistent with studies in other systems. For instance, ^{13}C-depletion of *ai*-C15:0 was linked to the involvement of SRB in AOM in the surface sediments of the Mediterranean ridge (δ^{13}C of $\sim -68‰$; Pancost et al. 2000), Black Sea sediments (δ^{13}C of $\sim -83.5‰$ to $-78.9‰$; Blumenberg et al. 2004), and sediments in freshwater Lake Cadagno, Switzerland (δ^{13}C, down to $-44.8‰$; Schubert et al. 2011).

To identify the potential ANME partners of SRB involved in AOM in Lake Kivu, Pasche et al. (2011) used methyl coenzyme M reductase (*mcrA*) genes as markers for ANME (as well as methanogens) and reported that the sequenced clones within the sulfate reducing zone (90 m) were most closely related to the *Methanomicrobiales* (potentially a new ANME group). Also, in the deeper anoxic regions (below 90 m) of the lake, Pasche et al. (2011) observed *mcrA* gene sequences that were most closely related to the ANME-2ab clade. In our study, we used probes for known ANME-1 and ANME-2 (Blumenberg et al 2004) but did not detect these in the lake (Fig. 8a), consistent with Pasche et al.'s (2011) observation that a novel cluster of ANME may be involved in AOM in the lake.

We detected archaeal cells (Figs. 8, 9) and the biomarker archaeol (Fig. 6a) in the anoxic region of the lake. The observed predominance of bacteria (57–81% of total DAPI

stained cells) over archaea (1–12% of total DAPI stained cells) throughout Lake Kivu agrees with Llirós et al. (2010), who reported bacterial (46–95% of total DAPI stained cells) vs. archaeal (0.3–4.6% of total DAPI stained cells) proportions in the surface and intermediate waters (0–100 m) of Lake Kivu, and is also consistent with observation in other freshwater lakes (Llirós et al. 2011). Archaeol is a diagnostic membrane lipid of archaea including methanogenic and methanotrophic archaea (Niemann and Elvert 2008). The isotopic composition of archaeol was moderately ^{13}C-depleted and not conclusive as to the predominant source of the archaeol.

To gain more insights into the predominant source of archaeol in the SPM, we used the distribution of archaea-derived isoprenoid GDGTs (isoGDGTs). While the isoGDGTs can be derived from crenarcheota, methanogenic archaea, and methanotrophic archaea (Blumenberg et al. 2004; Schouten et al. 2013), methanogenic archaea produce predominantly and sometimes only GDGT-0 (Blaga et al. 2009; Schouten et al. 2013). Values < 1 of the ratio of GDGT-0 to GDGT-IV and GDGT-0 to isoGDGT (Fig. 6b) indicate relatively lesser contributions from methanogenic archaeal lipids compared to lipids from crenarchaeota and other archaea groups (e.g., *Thaumarchaeota*) throughout the water column. The increased values of the ratios of GDGT-0 to GDGT-IV and GDGT-0 to isoGDGT with depth (Fig. 6b), and their higher values in the anoxic region imply higher contributions from methanogenic archaeal lipids in the anoxic region, in agreement with the reported biological origin of methane in the lake (Pasche et al. 2011). Llirós et al. (2010, 2012), in their study of the archaea community in Lake Kivu, noted that the phylotypes affiliated with the phyla Crenarchaeota, Thaumarchaeota, and Euryarchaeota comprised 32%, 43%, and 25% of the assigned operational taxonomic units. Consistent with our observation, they noted that most of the Crenarchaeota and Thaumarchaeota in the lake were from ammonia oxidizing archaea, whereas most of the Euryachaeota from the anoxic water column were from methanogens (*Methanosarcinales* and *Methanocellales*).

Isotope fractionation during methane oxidation and mixed-source contribution to methanotrophic biomarkers

Isotopic fractionation during biomass synthesis by MOB is reported to range from 3–39‰ and is influenced by the type of MOB (I, X, or II), dissolved CH_4 concentrations, cell densities, and the availability of copper (Summons et al. 1994; Jahnke et al. 1999; Templeton et al. 2006). While type I MOB synthesizes its biomass from CH_4-derived formaldehyde through the RuMP pathway, the type X MOB, in addition to using formaldehyde, is capable of using small amounts of CO_2 for biomass synthesis through the ribulose bisphosphate carboxylase pathway. In contrast, type II MOB, however, synthesizes 50–70% of its biomass from formaldehyde using the serine pathway, and produces 30–50% of its biomass from CO_2 using the phosphenolpyruvate carboxylase pathway (Hanson and Hanson 1996). These different pathways lead to varying isotopic fractionations in the different MOB. In their growth experiment studies of *Methylococcus capsulatus*, a type X MOB, Summons et al. (1994) reported an isotopic fractionation of 16–31‰ during growth, and Jahnke et al. (1999) observed a fractionation of $\sim$ 10‰ for the same species. In their experiments with pure cultures without copper amendments, Templeton et al. (2006) observed $\sim$ 14–24‰ and $\sim$ 1–13‰ ^{13}C-depletion of the biomass relative to substrate CH_4 by *Methylomonas methanica* (type I MOB) and *Methylosinus trichosporium* (type II MOB), respectively. They also observed that the biomass synthesized by *M. methanica* and *M. trichosporium* was 6‰ and 15‰ enriched in ^{13}C compared to the dissimilated CO_2. A much larger isotope fractionation (35–70‰) was reported to be associated with biomass synthesis by methanotrophic archaea during AOM (Blumenberg et al. 2004; Niemann and Elvert 2008).

In Lake Kivu, as the δ^{13}C of substrate CH_4 in the anoxic region of the lake was -62.6‰ to -56.6‰ (Fig. 4a), biomass from MOB directly consuming CH_4 would be on average ^{13}C-depleted by 16‰ relative to the source CH_4 (δ^{13}C of -78.6‰ to -72.6‰). Similarly, biomass from SRB and ANME involved in AOM is expected to be ^{13}C-depleted by at least 35‰ relative to the source CH_4 (δ^{13}C of -97.6‰ to -91.6‰). However, the biomarkers for type I MOB (fatty acids C16:1ω5, C16:1ω7), type II MOB (fatty acid C18:1ω7), and SRB partners of ANME (fatty acid *ai*-C15:0) were not as highly ^{13}C-depleted as should be the case if CH_4 was the only source of carbon. This implies that: (1) the MOB (especially type II MOB) were facultative (rather than obligate) methanotrophs, using other C1-compounds or substrates (e.g., CO_2) in addition to CH_4 for their biomass synthesis, which could lead to the observed ^{13}C-enrichment (or similarity) of the biomass relative to the source CH_4. (2) These PLFA biomarkers were derived from mixed sources. To further investigate the latter idea, we used a binary isotopic mixing model (Eq. 3) to tease apart the proportional contributions of methanotrophic lipids to the PLFA biomarkers. The model estimates indicate that 21–30% of the fatty acid *ai*-C15:0 in the SPM from the deep anoxic waters was derived from SRB involved in AOM. Also, lipids from type I MOB constituted 18–36% of the fatty acids C16:1ω7 and 40-50% of the fatty acid C16:1ω5 in the SPM from the anoxic waters of the lake. Finally, type II MOB contributed 32–38% of the fatty acid C18:1ω7 in the SPM from the oxic surface waters of the lake. It is worth noting that the fractionation factors previously published (and discussed above) for aerobic methanotrophs were from pure cultures and could be different in a mixed community under the prevailing environmental conditions in the lake.

This study showed that CH_4 in the water column of Lake Kivu was oxidized both anaerobically and aerobically, with anaerobic oxidation being a small sink for CH_4 compared to aerobic CH_4 oxidation in the lake. Molecular and isotopic data showed that aerobic CH_4 oxidation in the lake was mediated by type II MOB. Type I MOB were not involved in aerobic CH_4 oxidation in the surface waters but was involved in CH_4 oxidation in the anoxic deep waters of the lake. SRB were found in the deeper anoxic waters and were associated with AOM in the lake based on observed ^{13}C depletion of *ai*-C15:0 fatty acid. Methane constituted an important carbon and energy source (up to 38%) for the lake food web, including heterotrophic and autotrophic communities.

References

Amaral, J. A., and R. Knowles. 1995. Growth of methanotrophs in methane and oxygen counter gradients. FEMS Microbiol. Lett. **126**: 215–220. doi:10.1016/0378–1097(95)00012–T

Bastviken, D., J. Cole, M. Pace, and L. Tranvik. 2004. Methane emissions from lakes: Dependence of lake characteristics, two regional assessments, and a global estimate. Global Biogeochem. Cycles **18**: GB4009. doi:10.1029/2004GB002238

Bastviken, D., J. Ejlertsson, I. Sundh, and L. Tranvik. 2003. Methane as a source of carbon and energy for lake pelagic food webs. Ecology **84**: 969–981. doi:10.1890/0012–9658(2003)084[0969:MAASOC]2.0.CO;2

Beal, E. J., C. H. House, and V. J. Orphan. 2009. Manganese–and iron–dependent marine methane oxidation. Science **325**: 184–187. doi:10.1126/science.1169984

Blaga, C. I., G.–J. Reichart, O. Heiri, and J. S. S. Damsté. 2009. Tetraether membrane lipid distributions in water–column particulate matter and sediments: A study of 47 European lakes along a north–south transect. J. Paleolimnol. **41**: 523–540. doi:10.1007/s10933–008–9242–2

Blumenberg, M., R. Seifert, J. Reitner, T. Pape, and W. Michaelis. 2004. Membrane lipid patterns typify distinct anaerobic methanotrophic consortia. Proc. Natl. Acad. Sci. USA **101**: 11111–11116. doi:10.1073/pnas.0401188101

Bodelier, P. L., M. J. B. Gillisen, K. Hordijk, J. S. S. Damsté, W. I. C. Rijpstra, J. A. Geenevasen, and P. F. Dunfield. 2009. A reanalysis of phospholipid fatty acids as ecological biomarkers for methanotrophic bacteria. The ISME journal **3**: 606–617. doi:10.1038/ismej.2009.6

Boetius, A., and others. 2000. A marine microbial consortium apparently mediating anaerobic oxidation of methane. Nature **407**: 623–626. doi:10.1038/35036572.

Borges, A. V., G. Abril, B. Delille, J.–P. Descy and F. Darchambeau. 2011. Diffusive methane emissions to the atmosphere from Lake Kivu (Eastern Africa). J. Geophys. Res. **116**: G03032. doi:10.1029/2011JG001673

Crowe, S. A., S. Katsev, K. Leslie, A. Sturm, C. Magen, S. Nomosatryo, M. A. Pack, J. D. Kessler, W. S. Reeburgh, J. A. Roberts, L. Gonzalez, G. Douglas Haffner, A. Mucci, B. Sundby, and D. A. Fowle. 2011. The methane cycle in ferruginous Lake Matano. Geobiology **9**: 61–78. doi:10.1111/j.1472–4669.2010.00257.x

de Kluijver, A., P. L. Schoon, J. A. Downing, S. Schouten, and J. J. Middelburg. 2014. Stable carbon isotope biogeochemistry of lakes along a trophic gradient. Biogeosciences **11**: 6265–6276. doi:10.5194/bg-11-6265-2014

Daims, H., A. Brühl, R. Amann, K.–H. Schleifer, and M. Wagner. 1999. The domain–specific probe EUB338 is insufficient for the detection of all bacteria: Development and evaluation of a more comprehensive probe set. Syst. Appl. Microbiol. **22**: 434–444. doi:10.1016/S0723–2020(99)80053–8

Descy, J–P., F. Darchambeau, and M. Schmid. 2012. Lake Kivu research: Conclusions and perspectives, p. 181–190. In J.–P. Descy, F. Darchambeau, and M. Schmid [eds.], Lake Kivu, Springer

Durisch–Kaiser, and others. 2011. What prevents outgassing of methane to the atmosphere in Lake Tanganyika? J. Geophys. Res. **116**: G02022. doi:10.1029/2010JG001323

Eller, G., and P. Frenzel. 2001. Changes in activity and community structure of methane–oxidizing bacteria over the growth period of rice. Appl. Environ. Microbiol. **67**: 2395–2403. doi:10.1128/AEM.67.6.2395–2403.2001

Ettwig, K. F., and others. 2010. Nitrite–driven anaerobic methane oxidation by oxygenic bacteria. Nature **464**: 543–548. doi:10.1038/nature08883

Ettwig, K. F., S. Shima, K. T. Van De Pas–Schoonen, J. Kahnt, M. H. Medema, H. J. M. Op Den Camp, M. S. M. Jetten, and M. Strous. 2008. Denitrifying bacteria anaerobically oxidize methane in the absence of archaea. Environ. Microbiol. **10**: 3164–3173. doi:10.1111/j.1462–2920.2008.01724.x

Hanson, R. S., and T. E. Hanson. 1996. Methanotrophic bacteria. Microbiol. Rev. **60**: 439–471

Haroon, M. F., S. Hu, Y. Shi, M. Imelfort, J. Keller, P. Hugenholtz, Z. Yuan, and G. W. Tyson. 2013. Anaerobic oxidation of methane coupled to nitrate reduction in a novel archaeal lineage. Nature **500**: 567–570. doi:10.1038/nature12375

Hayes, J. M. 1993. Factors controlling ^{13}C content of sedimentary organic compounds: Principles and evidence. Mar. Geol. **113**: 111–125. doi:10.1016/0025–3227(93)90153–M

Jahnke, L. L., R. E. Summons, J. M. Hope, and D. J. Des Marais. 1999. Carbon isotopic fractionation in lipids from methanotrophic bacteria II: The effects of physiology and environmental parameters on the biosynthesis and isotopic signatures of biomarkers. Geochim. Cosmochim. Acta **63**: 79–93. doi:10.1016/S0016–7037(98)00270–1

Jannasch, H. W. 1975. Methane oxidation in Lake Kivu (central Africa). Limnol. Oceanogr. **20**: 860–864. doi:10.4319/lo.1975.20.5.0860

Julius, O. O. 2011. Trace metal pollution and physicochemical characteristics of Lake Kivu, Rwanda. Global J. Environ. Res. **5**: 57–64

Kankaala, P., S. Taipale, H. Nykänen and R. I. Jones. 2007. Oxidation, efflux, and isotopic fractionation of methane during autumnal turnover in a polyhumic, boreal lake. J. Geophys. Res. **112**: G02033. doi:10.1029/2006JG000336

Kirf, M., C. Dinkel, C. J. Schubert, and B. Wehrli. 2014. Submicromolar oxygen profiles at the oxic–anoxic boundary of temperate lakes. Aquat. Geochem. **20**: 39–57. doi:10.1007/s10498–013–9206–7

Knittel, K. and A. Boetius. 2009. Anaerobic oxidation of methane: progress with an unknown process. Annu. Rev. Microbiol. **63**: 311–334. doi:10.1146/annurev.micro.61.080706.093130

Kohring, L. L., D. B. Ringelberg, R. Devereux, D. A. Stahl, M. W. Mittelman, and D. C. White. 1994. Comparison of phylogenetic relationships based on phospholipid fatty acid profiles and ribosomal RNA sequence similarities among dissimilatory sulfate–reducing bacteria. FEMS Microbiol. Lett. **119**: 303–308. doi:10.1111/j.1574–6968.1994.tb06905.x

Lidstrom, M. E., and L. Somers. 1984. Seasonal study of methane oxidation in Lake Washington. Appl. Environ. Microbiol. **47**: 1255–1260

Llirós, M., and others. 2010. Vertical distribution of ammonia–oxidizing crenarchaeota and methanogens in the epipelagic waters of Lake Kivu (Rwanda–Democratic Republic of the Congo). Appl. Environ. Microbiol. **76**: 6853–6863. doi:10.1128/AEM.02864–09

Llirós, M., L. Alonso-Sáez, F. Gich, A. Plasencia, O. Auguet, E. O. Casamayor, C. M. Borrego. 2011. Active bacteria and archaea cells fixing bicarbonate in the dark along the water column of a stratified eutrophic lagoon. FEMS Microbiol. Ecol. **77**: 370–384. doi:10.1111/j.1574-6941.2011.01117.x

Llirós, M., and others. 2012. Microbial ecology of Lake Kivu, p. 85–105. In J.–P. Descy, F. Darchambeau, and M. Schmid [eds.], Lake Kivu, Springer

McCallister, S. L. and P. A. del Giorgio. 2008. Direct measurement of the $\delta^{13}C$ signature of carbon respired by bacteria in lakes: Linkages to potential carbon sources, ecosystem baseline metabolism, and CO_2 fluxes. Limnol. Oceanogr. **53**: 1204–1216. doi:10.2307/40058245

Milucka, J., and others. 2012. Zero–valent sulphur is a key intermediate in marine methane oxidation. Nature **491**: 541–546. doi:10.1038/nature11656

Morana, C., and others. 2014. Biogeochemistry of a large, meromictic tropical lake (Lake Kivu, East Africa): insights from a stable isotope study covering an annual cycle. Geophys. Res. Abstracts **16**: EGU2014–5086. doi:10.5194/bgd–11–17227–2014

Muvundja, F. A. 2010. Riverine nutrient inputs to Lake Kivu. M.S. thesis. Univ. of Makerere

Neef, A. 1997. Application of in situ single–cell identification of bacteria for population analysis in complex microbial biocoenosis. Ph.D. thesis. Technische Universität München

Niemann, H., and M. Elvert. 2008. Diagnostic lipid biomarker and stable carbon isotope signatures of microbial communities mediating the anaerobic oxidation of methane with sulphate. Org. Geochem. **39**: 1668–1677. doi:10.1016/j.orggeochem.2007.11.003

Pasche, N., C. Dinkel, B. Müller, M. Schmid, A. Wüest, and B. Wehrli. 2009. Physical and biogeochemical limits to internal nutrient loading of meromictic Lake Kivu. Limnol. Oceanogr. **54**: 1863–1873. doi:10.4319/lo.2009.54.6.1863

Pasche, N. and others. 2011. Methane sources and sinks in Lake Kivu. J. Geophys. Res. **116**: G03006. doi:10.1029/2011JG001690

Pancost, R. D., J. S. S. Damsté, S. De Lint, M. J. Van Der Maarel, and J. C. Gottschal. 2000. Biomarker evidence for widespread anaerobic methane oxidation in Mediterranean sediments by a consortium of methanogenic archaea and bacteria. Appl. Environ. Microbiol. **66**: 1126–1132. doi:10.1128/AEM.66.3.1126-1132.2000

Rahalkar, M., J. Deutzmann, B. Schink, and I. Bussmann. 2009. Abundance and activity of methanotrophic bacteria in littoral and profundal sediments of Lake Constance (Germany). Appl. Environ. Microbiol. **75**: 119–126. doi:10.1128/AEM.01350–08

Reeburgh, W. S. 2007. Oceanic methane biogeochemistry. Chem. Rev. **107**: 486–513. doi:10.1021/cr050362v

Rudd, J., and R. Hamilton. 1979. Methane cycling in Lake 227 in perspective with some components of carbon and oxygen cycles. Archiv für Hydrobiologie Ergebnisse der Limnologie **12**: 115–122

Sarmento, H., F. Darchambeau, M. Isumbisho, and J.–P. Descy. 2012. Phytoplankton of Lake Kivu, p. 67–83. In J.–P. Descy, F. Darchambeau, and M. Schmid [eds.], Lake Kivu, Springer

Schmid, M., M. Halbwachs, B. Wehrli, and A. Wüest. 2005. Weak mixing in Lake Kivu: New insights indicate increasing risk of uncontrolled gas eruption. Geochem. Geophys. Geosyst. **6**: Q07009. doi:10.1029/2004GC000892

Schmitz, M. 2011. Involvement of microbial populations in the nitrogen cycle in Lake Kivu. M.Sc. thesis, Univ. of Namur, Belgium

Schouten, S., E. C. Hopmans, and J. S. Sinninghe Damsté. 2013. The organic geochemistry of glycerol dialkyl glycerol tetraether lipids: A review. Org. Geochem. **54**: 19–61. doi:10.1016/j.orggeochem.2012.09.006

Schubert, C. J., J. Villanueva, S. E. Calvert, G. L. Cowie, U. von Rad, H. Schulz, U. Berner, H. Erlenkeuser. 1998. Stable phytoplankton community structure in the Arabian Sea over the past 200,000 years. Nature **394**: 563–566. doi:10.1038/29047

Schubert, C. J., and others. 2010. Oxidation and emission of methane in a monomictic lake (Rotsee, Switzerland). Aquat. Sci. **72**: 455–466. doi:10.1007/s00027–010–0148–5

Schubert, C. J., F. Vazquez, T. Losekann–Behrens, K. Knittel, M. Tonolla, and A. Boetius. 2011. Evidence for anaerobic oxidation of methane in sediments of a freshwater system (Lago di Cadagno). FEMS Microbiol. Ecol. **76**: 26–38. doi:10.1111/j.1574–6941.2010.01036.x

Stahl, D. A. and R. Amann. 1991. Development and application of nucleic acid probes, p. 205–248. In E. Stackebrandt and M. Goodfellow [eds.], Nucleic acid techniques in bacterial systematics. Wiley

Summons, R. E., L. L. Jahnke, and Z. Roksandic. 1994. Carbon isotopic fractionation in lipids from methanotrophic bacteria: Relevance for interpretation of the geochemical record of biomarkers. Geochim. Cosmochim. Acta **58**: 2853–2863. doi:10.1016/0016–7037(94)90119–8

Tavormina, P. L., W. Ussler, J. A. Steele, S. A. Connon, M. G. Klotz, and V. J. Orphan. 2013. Abundance and distribution of diverse membrane–bound monooxygenase (Cu–MMO) genes within the Costa Rica oxygen minimum zone. Environ. Microbiol. Rep. **5**: 414–423. doi:10.1111/1758–2229.12025

Templeton, A. S., K.–H. Chu, L. Alvarez–Cohen, and M. E. Conrad. 2006. Variable carbon isotope fractionation expressed by aerobic CH4–oxidizing bacteria. Geochim. Cosmochim. Acta **70**: 1739–1752. doi:10.1016/j.gca.2005.12.002

Treude, T., J. Niggemann, J. Kallmeyer, P. Wintersteller, C. J. Schubert, A. Boetius, and B. B. Jørgensen. 2005. Anaerobic oxidation of methane and sulfate reduction along the Chilean continental margin. Geochim. Cosmochim. Acta **69**: 2767–2779. doi:10.1016/j.gca.2005.01.002

Wakeham, S. G., J. I. Hedges, C. Lee, M. L. Peterson, and P. J. Hernes. 1997. Compositions and transport of lipid biomarkers through the water column and surficial sediments of the equatorial Pacific Ocean. Deep Sea Research II **44**: 2131–2162. doi:10.1016/S0967–0645(97)00035–0

Wallner, G., R. Amann, and W. Beisker. 1993. Optimizing fluorescent in situ hybridization with rRNA–targeted oligonucleotide probes for flow cytometric identification of microorganisms. Cytometry **14**: 136–143. doi:10.1002/cyto.990140205

Werne, J. P., M. Baas, and J. S. S. Damsté. 2002. Molecular isotopic tracing of carbon flow and trophic relationships in a methane–supported benthic microbial community. Limnol. Oceanogr. **47**: 1694–1701. doi:10.4319/lo.2002.47.6.1694

Whiticar, M. J. 1999. Carbon and hydrogen isotope systematics of bacterial formation and oxidation of methane. Chem. Geol. **161**: 291–314. doi:10.1016/S0009–2541(99)00092-3]

Acknowledgments

We thank Natacha Pasche (Lake Kivu Monitoring program, Ministry of Infrastructure, Gisenyi, Rwanda) for her assistance in field campaign preparations and during the campaign on Lake Kivu, Susan Lang (Swiss Federal Institute of Technology, Zurich) for the dissolved inorganic carbon (DIC) isotope analysis, Francien Peterse (Swiss Federal Institute of Technology, Zurich) for glycerol dialkyl glycerol tetraethers (GDGT) analysis, Gijs Nobel (deceased) for lab assistance during sample processing at Eawag, Switzerland, Elizabeth Minor, Josef Werne, the associate editor and two anonymous reviewers for their valuable comments on the manuscript. This work was funded by the Swiss National Science Foundation (20021–135299).

Submitted 13 March 2014
Revised 5 November 2014
Accepted 27 November 2014

Associate editor: Mary I. Scranton